Multiple PLCβ signaling pathways in taste receptor cells contribute to the detection of bitter, sweet and umami stimuli

Debarghya Dutta Banik[1], Eric D. Benfey[1], Laura E. Martin[2], Kristen E. Kay[2], Gregory C. Loney[2], Amy R. Nelson[1], Zachary C. Ahart[1], Barrett T. Kemp[1], Bailey R. Kemp[1], Aurelie Vandenbeuch[3], Ann-Marie Torregrossa[2,4] and Kathryn F. Medler*[1]

[1]Department of Biological Sciences, University at Buffalo, Buffalo, NY 14260, USA.

[2]Department of Psychology, University at Buffalo, Buffalo, NY 14260, USA.

[3]Department of Otolaryngology, University of Colorado, Aurora, CO, USA

[4]Center for Ingestive Behavior Research, University at Buffalo, Buffalo, NY 14260, USA

*Corresponding author: Email: kmedler@buffalo.edu

Summary: This study identifies a new role for PLCβ3 in the transduction of bitter, sweet and umami taste stimuli and demonstrates that multiple taste cell populations respond to these stimuli.

ABSTRACT

Taste receptor cells use multiple signaling pathways to detect chemicals. While salty and sour stimuli bind ion channels, bitter, sweet and umami stimuli activate a GPCR/PLCβ2/IP_3R3 signaling pathway. Current thinking is that all bitter, sweet and umami stimuli are detected by Type II cells via a PLCβ2/IP_3R3 pathway. Using live cell calcium (Ca^{2+}) imaging on isolated taste receptor cells from mice lacking IP_3R3 in Type II cells, we find many taste cells still robustly respond to bitter, sweet and umami stimuli, including a subset of Type III taste cells. Immunohistochemical analysis reveals that PLCβ3 is not expressed in Type II cells but is present in other taste cell populations, including a subset of Type III cells. Loss of either IP_3R3 or PLCβ3 in taste receptor cells cause comparable reductions in c-Fos labeling in the nucleus of the solitary tract following oral infusion of quinine. Short term behavioral assays also demonstrate that loss of either IP_3R3 from Type II cells or loss of PLCβ3 causes similar taste deficits, indicating that both molecules are required for normal taste transduction. Our data identify a critical, and previously unknown, role for PLCβ3 in taste transduction and demonstrate that input from multiple PLCβ pathways/taste receptor cell populations are required to transduce bitter, sweet and umami stimuli.

SIGNIFICANCE STATEMENT

It is currently thought that the transduction of bitter, sweet and umami stimuli in taste cells depends solely on GPCR/PLCβ2/IP_3R3 signaling in Type II taste receptor cells. However, in the absence of either PLCβ2 or IP_3R3, mice have reduced, but not abolished, ability to detect these stimuli, suggesting that other taste cells also contribute to taste transduction. When IP_3R3 is absent, Type II cells do not generate a Ca^{2+} signal to these taste stimuli; however, other taste receptor cells respond to bitter, sweet and umami stimuli, including a subset of Type III cells. We identified a PLCβ3 pathway that is expressed in non-Type II taste cells, including a subset of Type III cells. Loss of PLCβ3 significantly reduced taste cell responses, cFos-labeling in the nucleus of the solitary tract, and caused significant behavioral deficits. We conclude that PLCβ3 has an important role in taste transduction.

Chemicals in the oral cavity are detected by taste receptor cells which are grouped together in taste buds found in epithelial specializations in the tongue called papillae. There are three main papillae: Circumvallate (CV), foliate (Fol), and fungiform (Fun) which differ in their localization on the tongue and innervation by the cranial nerves. Despite these differences, taste papillae all house taste buds that are comprised of distinct cell types that vary in their signaling functions within the bud (1).

The current view of taste transduction is that taste buds are comprised of Type I, Type II and Type III taste receptor cells (2). Type I cells are thought to primarily function as support cells and share some characteristics of glia cells (3), while Type II cells detect bitter, sweet or umami stimuli through the activation of specific GPCRs for each of these taste qualities. The subsequent transduction of these taste qualities within the cells are due to a single signaling pathway that is comprised of phospholipase Cβ2 (PLCβ2) that activates the inositol 1,4,5-trisphosphate receptor type 3 (IP_3R3) on the endoplasmic reticulum to cause Ca^{2+} release (4-6). This Ca^{2+} release activates the transient receptor potential cation channel subfamily M members 4 and 5 (TRPM4 and TRPM5) which depolarize the cell sufficiently to activate the release of ATP through the calcium homeostasis modulator 1 (CALHM1) channel (5, 7-11). The expression of PLCβ2, IP_3R3 and TRPM5 is restricted to Type II taste cells within the bud and these cells lack both voltage-gated calcium channels (VGCCs) and conventional chemical synapses (model shown in Figure 1A)(12-16). Type III cells detect sour and salt stimuli through ionotropic receptors that depolarize the cell to activate VGCCs and cause vesicular neurotransmitter release (17-23) (see Figure 1A). It is currently thought that Type III cells do not respond to bitter, sweet or umami stimuli.

While this is the widely accepted view of signal transduction in peripheral taste cells, multiple genetic studies have reported that the deletion of individual signaling proteins in Type II cells, including PLCβ2, IP_3R3 and TRPM5, does not abolish the ability to detect all bitter sweet and umami stimuli (24-28). Similarly, the loss of Type II cells leads to severely reduced, but not abolished, responses to bitter, sweet and umami stimuli (29). These studies support the idea that additional signaling pathways are present in taste cells, but to date, few studies have focused on identifying these alternatives (30, 31). We previously reported that some taste cells generate Ca^{2+} responses to a bitter stimulus and cell depolarization, suggesting that taste cells with VGCCs, presumably Type III cells, respond to at least one bitter compound (32). A separate report also found some taste cells with VGCCs can respond to bitter stimuli (19). These studies led us to hypothesize that in addition to Type II cells, a separate population of taste cells may contribute to the detection of bitter, sweet and umami stimuli. To test this hypothesis, we used live cell imaging in mice that lack IP_3R3 and found that many taste cells still responded to bitter, sweet and umami stimuli, including a subset of Type III cells. These cells responded to taste stimuli through a distinct PLCβ which we identified as PLCβ3. We conclude that multiple populations of taste cells use distinct signaling pathways to respond to bitter, sweet and umami stimuli.

RESULTS

Bitter, sweet and umami taste evoked responses are still present in IP_3R3-KO mice

IP_3R3 is part of the canonical signaling pathway in Type II cells that respond to bitter, sweet and umami stimuli and its expression is localized in Type II cells (4, 12, 16, 33). One study using single cell PCR reported mRNA levels for IP_3R3 in both Type II cells and some SNAP25+ cells (a Type III marker) but did not evaluate protein expression for these compounds (34). In contrast, another study using an IP_3R3-GFP mouse reported that GFP+ cells did not functionally express VGCCs, a physiological marker for Type III cells (32). While these conflicting reports suggest that it is possible that IP_3R3 expression is not restricted to Type II cells, for the purposes of our current study, we are presuming that IP_3R3 is only expressed in Type II cells.

To evaluate the taste evoked signaling in taste receptor cells that lack the ability to release Ca^{2+} via IP_3R3, we used a transgenic mouse in which GFP replaces the coding region of IP_3R3. In these mice, GFP labels the cells that should express IP_3R3 but no longer do so. Initial immunohistochemical analyses found that taste cells from the CV papillae of wild type mice were successfully labeled with anti-IP_3R3 antibody (n=3; Figure S1A), while their KO littermates lacked IP_3R3 labeling but instead have GFP expression (n=6; Figure S1B). Furthermore, anti-IP_3R3 labels the GFP expressing cells in IP_3R3-heterzygous mice (n=4; Figure S1C); confirming that GFP expression identifies the taste cells that normally express IP_3R3. To further characterize this mouse, we evaluated the expression of other proteins that are part of this established signaling pathway in Type II cells. The GFP expression in the KO mice co-localized with both PLCβ2 (n=4; Figure S1D) and gustducin (n=3; Figure S1E) labeling. As expected, gustducin expression was restricted to the IP_3R3-GFP-KO cells but not all GFP expressing cells had gustducin while there was complete overlap between PLCβ2

labeling and GFP. Co-localization analyses are reported in Figures S1F. Thus the other components of the signaling pathway normally found in Type II cells are intact but these cells no longer have the capacity to release Ca^{2+} in response to bitter, sweet or umami stimuli.

We evaluated this IP_3R3-GFP-KO mouse using Fura2-AM to measure the taste-evoked Ca^{2+} responses in taste receptor cells. All measurements were made in isolated taste cells that were no longer associated with the taste bud to ensure that the taste-evoked Ca^{2+} responses were due solely to the activity of the individual taste cells and not cell-to-cell communication (example in Figure 1B, C). We applied multiple bitter, sweet and umami stimuli as well as 50mM KCl to isolated cells from CV, Fol or Fun papillae of the wild type and IP_3R3-KO mice. Since our goal was to identify all (or most) responsive taste cells, we used the stimulus concentration that generated a maximal Ca^{2+} signal. These concentrations were based on control experiments we used to identify the lowest stimulus concentration that generated the maximal Ca^{2+} signal (examples shown in Figure S2, A-C). This increased our likelihood of identifying responsive taste cells but did not generate any non-specific responses (Figure S2, D, E). As shown in Figure S2C, a GFP+ cell did not respond to any concentration of stimulus applied. Thus, the taste cells respond to a wide range of stimulus concentrations and the reported responses are not due to a concentration or osmotic effect.

We reasoned that if the Type II cells were solely responsible for all bitter, sweet and umami taste transduction, then the loss of IP_3R3 in Type II cells would abolish all Ca^{2+} responses to bitter, sweet and umami stimuli. In the IP_3R3-KO mice, GFP-

expressing cells lack IP_3R3 and did not respond to any taste stimuli tested (n=80, Figure 2B, S2C); however, a large number of non-GFP expressing taste cells responded to the stimuli. Initially, the response frequencies *(total number of responsive cells/total number of cells stimulated*) were measured for all taste cells from the wild type (WT) and IP_3R3-KO mice, including both GFP+ and GFP- cells (Figure 2A). The table in Figure 2A reports the taste response frequencies in wild type (WT) and IP_3R3-KO mice with the GFP+ cells included in the analysis. Not all cells were exposed to all stimuli and some cells responded to multiple stimuli. These experimental conditions preclude the data from being additive, so we compared the frequency of responses for a given stimulus between the wild type and IP_3R3-KO mice. These data demonstrate that the overall responsiveness to bitter, sweet, and/or umami stimuli was significantly reduced ($p<0.0001$) in the KO mice compared to WT cells. The likelihood that taste cells from CV would respond to taste stimuli was significantly reduced ($p=0.0003$). The responsiveness of the taste cells from the Fol and Fun papillae was not significantly affected by the loss of IP_3R3, even though the GFP+ cells were included in this analysis.

To further characterize the response profiles of the non-Type II taste cells, we analyzed the non-GFP expressing cells and plotted the response frequencies for each papillae and stimulus (Figure 2B-E). The GFP+ cells were not included in these response analyses and descriptions of the different taste cell populations are shown in Supplementary Table 1. Figure 2B compares the overall percent responsiveness of WT and KO mice for each papillae type (without the GFP+ cells) while the graphs in Figures 2C-E show the percentage of responsive cells in each papillae type for each specific

stimulus applied. The overall responsiveness of taste cells was only significantly reduced in the CV papillae when IP_3R3 was absent ($p<0.01$). Analysis of the individual stimuli for each papillae type (Figures 2C-E) identified significant reductions in the responsiveness to the sweet stimuli tested in the KO mice. Individual cell numbers are provided in Figure S3. Therefore, removing a key protein in the canonical GPCR/PLCβ2/IP_3R3 signaling pathway in Type II cells does not eliminate the ability of all taste cells to generate Ca^{2+} signals when stimulated by bitter, sweet or umami stimuli. Based on these data, we hypothesize there are additional signaling pathways that respond to these stimuli.

Bitter, sweet and umami stimuli are dependent on a PLCβ signaling pathway in IP_3R3-KO mice

To identify the type of signaling pathway that generates the taste responses in the non-GFP cells in the IP_3R3-KO mice, we analyzed bitter (5mM Den), sweet (20mM sucrose) and umami (10mM MPG) stimuli and found they generated signals in Ca^{2+}-free Tyrode's, indicating these signals depend on Ca^{2+} release from internal stores (Figure 3A,D,G). We confirmed these results by applying thapsigargin to disrupt the internal Ca^{2+} stores which abolished the taste evoked Ca^{2+} signals (Figure 3B,E,H). These responses were also eliminated when the general PLC blocker U73122 was applied (Figure 3C,F,I), indicating that these taste evoked Ca^{2+} responses in the IP_3R3-KO mice are due to the activation of another PLC signaling pathway. Individual data points for each experiment are shown in Figure S4.

PLCβ3 expression in peripheral taste cells

To identify other PLCβ isoforms expressed in taste receptor cells, we analyzed previously published RNAseq data (35). We found that PLCβ2 and PLCβ3 were expressed at comparable levels and were the predominant PLCβ isoforms present in taste cells. Therefore, we investigated the possibility that PLCβ3 is expressed in peripheral taste cells. Immunohistochemical experiments in the IP_3R3-KO mouse revealed strong PLCβ3 labeling that was separate from the Type II cells (identified with GFP expression) in the CV, Fol and Fun papillae (Figure 4A-C). Colocalization analysis is shown in Figure 4D. These data were confirmed using both the TRPM5-GFP mouse as well as co-labeling with PLCβ2 in C57BL/6 mice (Type II cell markers, Figure S5A, B, colocalization analysis shown in S5D). Co-labeling with the Type I taste marker NTPDase2 found that PLCβ3 is also not expressed in Type I cells (Figure S5C). We used qPCR to measure the relative amounts of mRNA for PLCβ3 and PLCβ2 in the different papillae (Figure S5E,F) and found that both PLCβ2 and PLCβ3 are expressed in CV, Fol and Fun papillae. We conclude that both PLCβ2 and PLCβ3 are highly expressed in peripheral taste cells but that PLCβ3 is not expressed in either Type I or Type II taste cells. Our next goal was to identify the cell population that expresses the PLCβ3 signaling pathway and responds to bitter, sweet and umami stimuli.

Some Type III cells respond to bitter, sweet and umami stimuli

The only other identified taste receptor cell type is the Type III cell. Type III cells are the only taste cell population that express VGCCs (36) and can be functionally identified in live cell imaging by the ability to respond to cell depolarization with a Ca^{2+} influx through the opening of VGCCs (19, 37). Earlier studies have reported that Type III cells are sour sensitive and that a subset of the sour-sensitive Type III cells is also salt

196 sensitive (17, 19, 38). To functionally identify Type III cells, we applied 50mM KCl to
197 cause a cell depolarization which generated a Ca^{2+} signal if the cell expresses VGCCs.
198 Therefore, if a cell responded to 50mM KCl with a Ca^{2+} signal, we concluded that it
199 expresses VGCCs and identified it as a Type III cell. We found that some Type III taste
200 cells in the IP_3R3-KO mouse responded to bitter, sweet and umami stimuli (Figure 5A-
201 C). To confirm that the taste cells that responded to 50mM KCl and bitter, sweet or
202 umami stimuli were Type III cells, we tested a subset of cells with sour (citric acid) and
203 salt (NaCl) stimuli (Figure 5D-F). All of the taste cells that responded to 50mM KCl
204 responded to citric acid with a Ca^{2+} signal (CA) while some of these cells also
205 responded to bitter, sweet and/or umami stimuli (Figure 5D, F). Interestingly, a
206 separate subset of 50mM KCl/CA cells responded to NaCl with a Ca^{2+} signal but were
207 not sensitive to the bitter, sweet, umami stimuli (Figure 5E, F). This indicates that the
208 sour/salt sensitive Type III cells are separate from the sour sensitive Type III cells that
209 respond to bitter, sweet and/or umami stimuli with a Ca^{2+} signal. Thus a subset of Type
210 III cells are dual responsive (DR) because they express VGCCs and are sour sensitive
211 but also respond to bitter, sweet and/or umami stimuli.

212 To determine if the loss of IP_3R3 in Type II cells affected the activity of DR cells,
213 we compared the percentage of cells that responded to any stimulus (bitter, sweet,
214 umami or 50mM KCl) in wild type and IP_3R3-KO mice. These data include all taste cells
215 from all three papillae taken from Figure 2A. As shown before, the overall
216 responsiveness to taste stimuli in the IP_3R3-KO mice was significantly reduced
217 compared to wild type (Figure 5G); however, the percentage of DR cells in the IP_3R3-
218 KO was not different from wild type mice (Figure 5G). Therefore, the ability of the DR

cells to respond to taste stimuli does not depend on the presence of IP_3R3 in Type II cells (Figure 5G, H).

We also performed control experiments using the GAD67-GFP mice as a cellular marker to identify Type III taste cells (39) and found that both GAD67-GFP positive and negative taste cells responded to taste stimuli + 50mM KCl with Ca^{2+} signals (Figure S6A-B). DR cells were also identified in C57BL/6 mice (Figure S6C). A recent study reported that some Type III cells from C57BL/6 mice responded to bitter stimuli (19) in agreement with our findings. Thus, DR Type III taste cells are present in taste cells in multiple mouse lines.

PLCβ3 contributes to taste evoked signaling in a subset of Type III cells

So far our data have identified that 1) there is a population of taste cells that do not depend on IP_3R3 (in Type II cells) to respond to bitter, sweet and umami, 2) PLCβ3 is expressed in taste cells, and 3) some Type III cells are DR and can respond to bitter, sweet and umami stimuli. We hypothesized that PLCβ3 is involved in the signaling of the DR cells. We next performed live cell imaging on isolated cells from CV, Fol, and Fun papillae of PLCβ3-KO and wild type mice to evaluate how the loss of PLCβ3 affects taste cell responsiveness, in particular the responsiveness of the DR cells. Loss of PLCβ3 resulted in significant reductions in the overall responsiveness of the PLCβ3-KO Fol and Fun cells but not the CV cells (Figure 6A,B). Knocking out PLCβ3 had a two-fold effect, it reduced the number of responses to bitter, sweet or umami stimuli and it significantly reduced the number of DR taste cells in CV, Fol and Fun taste cells (Figure 6C-E). Control experiments found no change in the ability of Type III cells to respond to sour or salt stimuli (Figure S7A-C). Type II cells were also still functional in PLCβ3-KO

mice (Figure S7D-F). Individual cell numbers are shown in Figure S8. These data indicate that PLCβ3 is contributing to the activity of the DR cells.

We next determined if PLCβ3 is expressed in Type III cells using SNAP-25 which is a synaptic protein that is a cellular marker for Type III taste cells (16, 40). Immunohistochemical analysis found some co-expression of PLCβ3 and SNAP25 in wild type mice (Figure S9A,B,E). There was no loss of SNAP-25 expression in the PLCβ3-KO mouse compared to WT (Figure S9C,D). Thus, PLCβ3 is expressed in some Type III cells and the loss of this protein did not affect the expression of SNAP25 in Type III cells.

The significant reduction in the number of taste evoked Ca^{2+} responses in the DR cells from PLCβ3-KO mice suggests that PLCβ3 is responsible for transducing most of the taste-evoked responses in these cells. To determine if the loss of both IP_3R3 and PLCβ3 would completely abolish the ability to respond to bitter, sweet and umami stimuli, we attempted to generate a double knock out mouse by breeding the IP_3R3-KO and PLCβ3-KO mice but the mice were not viable.

Loss of PLCβ3 causes deficits in the taste-evoked activity in the nucleus of the solitary tract.

To determine if the loss of IP_3R3 or PLCβ3 in taste cells affected the taste signal that is sent to the brain, we measured the neural activity in the nucleus of the solitary tract (NTS) using c-Fos labeling as a marker for activated neurons. This approach is commonly used to identify recently activated neurons, including neurons in the taste pathway (41-45). The NTS receives input from the gustatory neurons and is the first synaptic relay from the peripheral taste system. Mice (n=3 for each condition) were

orally infused with quinine (5mM) or water for 30 min. The level of c-Fos labeling for both IP_3R3-KO and PLCβ3-KO mice were compared to WT and water controls. Loss of either of these proteins resulted in a significant reduction in c-Fos activity to a level that was comparable to water (Figure 7). Control experiments demonstrate that neither IP_3R3 nor PLCβ3 are expressed in this region of the NTS (Figure S10).

Loss of PLCβ3 significantly affects taste-driven licking for bitter, sweet and umami

We then performed brief-access licking experiments to determine if the loss of taste-evoked signals in the PLCβ3-KO mice correlated with loss of taste sensitivity. Measurements were also made with IP_3R3-KO mice for comparison. Since the PLCβ3-KO mouse has a mixed genetic background while the IP_3R3-KO mice are in a C57BL/6 background, wild type littermates for both mouse lines were used as controls (Figure 8). The wild type mice both demonstrated concentration dependent decreases in licking to denatonium while PLCβ3-KO and IP_3R3-KO mice treated the solution similarly to water except for the highest concentration (20mM Den, Figure 8A). Wild type mice treated MSG (+ 10μM amiloride) solutions as more palatable than water up to 400mM and then decreased licking at the highest concentrations (600 and 800mM, Figure 8B). Both of the KO mice treated MSG like water. In the brief access test for the artificial sweetener, Acesulfame K (AceK), wild type mice increased licking up to 2 mM and then decreased licking at higher concentrations. Neither of the KO mice had a comparable concentration dependent change in licking (Figure 8C). Because sucrose is hedonically positive under wild type conditions, the lick score is calculated as licks to the stimulus minus licks to water, therefore a score close to zero resembles water. Neither the PLCβ3-KO nor

288 IP_3R3-KO mice showed a concentration-dependent effect on licking to sucrose until
289 they were presented with the highest concentration. In contrast, both sets of wild type
290 mice showed strong concentration dependent increases in licking to sucrose (Figure
291 8D). For the salt stimulus (NaCl), there were no significant differences in the licking
292 behavior for either of the KO mice compared to wild type mice, indicating that the ability
293 to respond to salt is not affected by loss of either PLCβ3 or IP_3R3 (Figure 8E). Thus
294 loss of either IP_3R3 or PLCβ3 caused comparable, and almost complete, loss of
295 preference for the bitter, sweet and umami stimuli tested but not salt taste.

296 **Response profiles for the dual-responsive taste cells**

297 Finally, we analyzed *how* DR cells respond to taste stimuli. We evaluated a
298 subset of DR cells that were stimulated with at least one bitter, one sweet and one
299 umami stimulus *and responded* to at least one of these stimuli. If the DR cells were not
300 stimulated with all three types of taste qualities, they were excluded from this analysis.
301 We created response profiles for bitter, sweet and umami in wild type and IP_3R3-KO
302 mice (Figure S11A-C) and found that the DR taste cells were most likely to be broadly
303 tuned (respond to all three types of stimuli). Few, if any, of the DR cells responded to a
304 single taste quality (in addition to 50mM KCl). We found that the loss of IP_3R3 did not
305 influence these response profiles.

306 **Three populations of taste cells respond to bitter, sweet and umami stimuli**

307 We repeated the same analysis on taste cells from wild type and IP_3R3-KO mice
308 that were stimulated with bitter, sweet, umami and 50mM KCl but *did not respond to*
309 *50mM KCl* (Figure S11D-F). Therefore, wild type taste cells analyzed included all the
310 Type II taste cells as well as any other taste cells that responded to bitter, sweet and/or

umami stimuli but lack VGCCs. We only analyzed taste cells that responded to at least one of these stimuli and compiled a response profile for these taste cells from wild type and IP_3R3-KO mice. These taste cells were much less likely to be broadly tuned in both the WT and KO taste cell populations.

While the taste-only cells from wild type mice express IP_3R3 and therefore should have Type II cells contributing to these response profiles, the analysis of the IP_3R3-KO mice was focused on taste cells that were not functional Type II taste cells (due to the absence of IP_3R3). These cells also did not respond to 50mM KCl with a Ca^{2+} signal and are not Type III cells. Therefore, this taste cell population lacks functional Type II cells and VGCCs but responds to bitter, sweet and/or umami stimuli. These functional data suggest that there are at least three populations of taste cells that can respond to bitter, sweet and umami stimuli: 1) Type II cells (identified as cells using IP_3R3), 2) a subset of Type III cells (which respond to 50mM KCl with a Ca^{2+} signal) and 3) another population of taste cells that are not Type II or Type III cells (neither reliant on IP_3R3 nor responsive to 50mM KCl). Future studies are needed to identify and characterize this taste cell population.

DISCUSSION

Our data establish that PLCβ3 signaling in taste receptor cells is important in the detection of bitter, sweet and umami taste stimuli. The presence of a second signaling pathway that detects these stimuli resolves a long standing inconsistency in the taste field. One study concluded that the PLCβ2 signaling pathway in Type II cells is entirely responsible for the detection of bitter, sweet and umami stimuli (5). A second study focused on understanding the role of Skn-1a in taste cell formation reported that the

loss of Skn-1a caused a significant remodeling of the taste bud. Using *in situ* hybridization, the authors did not detect the canonical signaling molecules normally found in Type II cells but did identify an increase in the Type III cell marker expression. They also reported significant behavioral and gustatory nerve defects for bitter, sweet and umami stimuli in the absence of Skn-1a, indicating that Type II cells are required to detect these stimuli (29). However, other studies reported that knocking out any component of the GPCR/PLCβ2/IP_3R3 pathway resulted in reduced, but not abolished, signaling for these stimuli (24-28, 46-49). There are deficits in taste-evoked signaling when any part of the GPCR/PLCβ2/IP_3R3 pathway is nonfunctional, but they are variable and there was never complete abolishment of the responses. Nevertheless, the current dogma within the taste field is that only this signaling pathway is responsible for all bitter, sweet and umami transduction (5). While this is puzzling, it is likely due to the lack of another identified signaling pathway that transmits taste signals. We have now identified that a PLCβ3 signaling pathway also detects bitter, sweet and umami stimuli.

Indeed, a closer inspection of the reported findings from these earlier studies reveals differential deficits in taste responses when the PLCβ2/IP_3R3 signaling pathway is nonfunctional. Evaluations of IP_3R3 loss in mice found impaired behavior and nerve responses to different taste stimuli, but not abolishment of these signals (25). They reported reduced behavioral sensitivity for bitter and sweet stimuli at some concentrations but no differences from controls at other concentrations. The cranial nerve recordings revealed deficits in signals that varied with the cranial nerve and taste stimulus being tested (25). These findings confirm that IP_3R3 is required for normal

taste signaling but also suggest that it is not the only pathway involved. Similarly, work focused on the loss of PLCβ2 reported reduced, but not abolished, avoidance of bitter compounds by PLCβ2-KO mice (28). In this study, the PLCβ2-KO mice did not avoid denatonium as well as wild type mice but still reduced licking as denatonium concentration increased. The PLCβ2-KO mice did not lick normally for sucrose but did lick normally for salt and sour stimuli. The authors concluded that a PLCβ2-independent pathway also contributes to taste transduction (28) which agrees with the IP_3R3-KO study (25). Other studies found that PLCβ2 and IP_3R3 co-localize (4, 12, 33) in Type II taste cells, so it is not surprising that loss of either protein causes similar deficits in taste-driven behaviors.

We measured the neural activity in the NTS using c-Fos labeling as a marker for activated neurons to determine how the loss of PLCβ3 affects central processing of taste information from the periphery (Figure 7). We used oral infusions of taste stimuli in awake and behaving animals because it removes any potential confounds due to anesthetization that is used in other approaches. Since the NTS receives input from the gustatory neurons and is the first synaptic relay from the peripheral taste system, these data confirm that loss of either IP_3R3 or PLCβ3 in the taste cells abolishes the taste signal that is sent to the brain. These data from the NTS agrees entirely with our behavioral data (Figure 8) which together support the idea that both IP_3R3 and PLCβ3 have important roles in taste transduction.

Loss of PLCβ3 caused significant behavioral impairments for the bitter, sweet and umami stimuli that were comparable to the behavioral deficits when IP_3R3 was not present in Type II cells. The loss of either protein was specific to these taste stimuli and

did not affect salt taste (Figure 8E). These data confirm that the lack of either IP_3R3 signaling in Type II or PLCβ3 signaling in taste cells had a comparable impact on taste behaviors (Figure 8). Since PLCβ3 and IP_3R3 are not expressed in the NTS (Figure S10) or the geniculate ganglia (50), these data strongly support the idea that input from both of these signaling molecules in taste cells is required for normal taste behavior. Therefore, if signaling from either population of taste cells (those using IP_3R3 or those using PLCβ3) is impaired, taste information is not properly conveyed to the brain. This conclusion agrees with other studies which suggest that Type II cells are not the only cells that transduce bitter, sweet and umami stimuli (24, 25, 27, 28).

Our data support the idea that multiple taste receptor mechanisms, outside of those canonically identified, are involved in the detection of different taste stimuli. Multiple laboratories have independently concluded that the identified taste receptors are not solely responsible for transducing all bitter, sweet and umami stimuli. For instance, the detection of some carbohydrates is not impaired by the loss of T1R2 or T1R3, the identified sweet receptors (47-49, 51), and umami stimuli appear to be transduced by receptors in addition to the T1R1+T1R3 heterodimer (31, 52-58). Moreover, because the identified T1Rs and T2Rs appear to have restricted expression in Type II taste cells (5, 59), the presence of the PLCβ3 signaling pathway in non-Type II cells bolsters the hypothesis that additional taste receptor mechanisms are likely involved in transduction.

Our data clearly demonstrate that a subset of Type III cells (DR) are sensitive to bitter, sweet and/or umami stimuli in contrast to the idea that Type III cells only detect sour and salty stimuli (19, 38). Furthermore, it appears likely that PLCβ3 is expressed

in Type III cells and is responsible for the bitter, sweet and umami responses recorded in a subset of Type III cells. We previously reported that a PLCβ3/IP_3R1 signaling pathway is expressed in a subset of taste cells that are not Type II cells (32) which our current data suggest is a subset of Type III cells. These physiological findings are supported by recent RNA-sequencing analysis of individual Type II and Type III cells (37) which revealed PLCβ3 expression in a subset of Type III cells.

We found that many of the DR Type III cells were broadly tuned and responded to two or more taste qualities, including taste stimuli of different modalities (Figure S6. S11). Importantly, our studies used isolated taste cells that were not in contact with neighboring cells. Earlier studies using intact buds or taste epithelium reported that a subset of taste cells responded to multiple stimuli with some of these studies concluding these cells likely received input from neighboring taste cells (60-62). While we do not rule out the possibility that taste cells receive input from other taste cells, our data show that DR Type III cells do not require neighboring input to respond to bitter, sweet or umami stimuli.

Our study has demonstrated that 1) Type II cells as defined by the expression of the IP_3R3 are not the *only* taste cells in the bud that detect bitter, sweet and umami stimuli; 2) taste cells with a PLCβ3 pathway also detect bitter, sweet and umami stimuli; 3) PLCβ3 is not expressed in Type II cells but is present in a subset of Type III cells and another population of taste cells that lack VGCCs; and 4) loss of either IP_3R3 or PLCβ3 in taste cells causes similar deficits in taste-dependent c-Fos activity in the NTS as well as deficits in taste driven behaviors. We conclude that peripheral taste transduction is more complex than is currently appreciated.

EXPERIMENTAL PROCEDURES

Mice

Animals were cared for in compliance with the University at Buffalo Institutional Animal Care and Use Committee. Multiple mouse lines were used in this study. Both sexes were used and mice ranged in age from 1 to 6 months. Taste cells for qPCR analyses were collected from C57BL/6 mice. The IP_3R3-KO mouse was generated in a C57BL/6 background and was obtained from the Mutant Mouse Resources and Research Center (MMRRC:032884-JAX). This mouse has a targeted mutation in which exon 1 is replaced with a MAPT/GFP fusion (63) which results in the expression of GFP in place of a functional IP_3R3 receptor. Thus, these mice lack a functional IP_3R3 receptor and express GFP in cells that would otherwise have expressed IP_3R3. Heterozygous mice express both GFP and the IP_3R3 receptor. The PLCβ3-KO mouse was generously provided by Dr. Sang-Kyou Han (64). The mutation in these mice disrupts the catalytic domain of phospholipase C and was generated in a 129SV agouti mouse strain that was crossed with CD1 mice (65). These mice were maintained in this mixed background. Immunohistochemical analyses were also performed in the TRPM5-GFP mouse strain which expresses GFP in all taste cells that express TRPM5. These mice have been backcrossed into the C57BL/6 background and were used as another marker of Type II taste cells (16) to evaluate the expression patterns of PLCβ3. These mice were generously provided by Dr. Robert Margolskee.

Taste Receptor Cell Isolation

Taste receptor cells were harvested from CV, Fol and Fun papillae of adult mice as previously described (32, 66-71). Briefly, mice were sacrificed using carbon dioxide

and cervical dislocation. Tongues were removed and an enzyme solution containing 0.7mg/mL Collagenase B (Roche, Basel, Switzerland), 3mg/mL Dispase II (Roche), and 1mg/mL Trypsin Inhibitor (Sigma-Aldrich, St. Louis, MO) was injected beneath the lingual epithelium. After the tongues were incubated in oxygenated Tyrode's solution for approximately 17 min, the epithelium was peeled from the underlying muscle and pinned serosal side up before it was incubated in Ca^{2+}-free Tyrode's for approximately 25 min. Cells were removed from taste papillae using capillary pipettes with gentle suction and placed onto coverslips coated with Cell-Tak (Corning, Corning, NY).

Ca^{2+} Imaging

All measurements of intracellular calcium (Ca^{2+}) were performed in isolated taste receptor cells that were no longer in contact with other taste cells. Cells were loaded for 20 minutes at room temperature (RT) with 2 μM Fura2-AM (Molecular Probes, Invitrogen, Carlsbad, CA) containing Pluronic F-127 (Molecular Probes). Loaded cells were then washed in Tyrode's solution under constant perfusion for 20min. Multiple taste stimuli and high potassium (50mM KCl) solutions were individually applied and Ca^{2+} responses were recorded. Cells were visualized using an Olympus IX73 microscope with a 40x oil immersion lens and images were captured with a Hamamatsu ORCA-03G camera (Hamamatsu Photonics K.K., SZK Japan). Excitation wavelengths of 340nm and 380nm were used with an emission wavelength of 510nm. Cells were kept under constant perfusion using a gravity flow perfusion system (Automate Scientific, San Francisco, CA). Images were collected every 4s using Imaging Workbench 6.0 (Indec Biosystems, Santa Clara, CA). Experiments were graphed and analyzed using Origin 9.2 software (OriginLab, Northhampton, MA).

Intracellular Ca^{2+} levels were measured as a ratio of fluorescence intensities. Fluorescence values were calibrated using the Fura-2 Ca^{2+} Imaging Calibration kit (Invitrogen). The effective dissociation constant K_d was calculated to be 180nM, which was used in the following equation to calculate Ca^{2+} concentration:

$$[Ca^{2+}] = K_d\,[(R-R_{min})/(R_{max}-R)](S_{f2}/S_{b2})$$

$$[Ca^{2+}] = 0.180\,[(R-0.338)/(26.81-R)](22.19)$$

R is the ratio value of fluorescence obtained after exciting cells at 340 and 380nm. Data from cells were analyzed if the cell had a stable Ca^{2+} baseline within the range of 65nM and 200nM. An evoked response was defined as measurable if the increase in fluorescence was at least two standard deviations above baseline.

Immunohistochemistry

Mice were deeply anesthetized by intraperitoneal injections of sodium pentobarbitol, 40 mg/kg (Patterson Veterinary, Mason, MI). Mice were then injected intracardially with heparin (Sigma) and 1% sodium nitrate (Sigma) followed by perfusion with approximately 30mL of 4% paraformaldehyde (Electron Microscopy Sciences, Ft. Washington, PA) in 0.1M phosphate buffer (PB), pH 7.2. After perfusion, the tongues were removed and placed in 4% paraformaldehyde/0.1M PB for 1-2h followed by a 4°C overnight incubation in 20% sucrose/0.1M PB, pH 7.2. For some experiments, tongues were immersion fixed overnight in 4% paraformaldehyde/0.1M PB, pH 7.2 at 4ºC with 20% sucrose. Regardless of the fixation method, the next day, 40μm sections were cut and washed in PBS 3X10 min at RT. For some experiments, antigen retrieval was performed by placing sections in 10 mM sodium citrate, pH 8.5 at 80°C for 5 min. This

was done to disrupt the cross-bridges formed by fixation and expose antigen binding sites.

Sections were incubated in blocking solution (0.3% Triton X-100, 1% normal goat serum and 1% bovine serum albumin in 0.1M PB) for 1-2h at RT. Primary antibody was added to the sections in blocking solution and incubated for 2 hours at RT followed by overnight exposure to primary antibody at 4°C. Controls with no primary antibody were included in each experiment. All primary antibodies were diluted in blocking solution. Mouse anti-IP_3R3 (Transduction Labs, Lexington, KY) was used at 1:50 following antigen retrieval. Rabbit anti-PLCβ3 (Abcam) was used at 1:200, rabbit anti-PLCβ2 (Santa Cruz Laboratories, Santa Cruz, CA) was used at 1:1000, rabbit anti-gustducin (Santa Cruz) was used at 1:200 and anti-NTPDase2 (1:100(72). Mouse anti-SNAP-25 (Genway Biotech, San Diego, CA) was used at 1:200 following antigen retrieval. Following overnight incubation in primary antibody, sections were washed in PBS 3X10 min at RT and then incubated with the appropriate secondary antibody (Cy5, 1:500; Rhod, 1:250; Jackson ImmunoResearch Laboratories, West Grove, PA) at RT for 2h in the dark. Controls were performed for double labeling experiments to ensure secondary antibodies were not binding to primary antibodies raised in different organisms. After secondary antibody incubation, sections were washed in PBS (3x10 min) and mounted on Superfrost Plus slides (VWR, Radnor, PA) using Fluoromount G (Southern Biotechnology Associates, Birmingham, AL) and coverslipped. All images were obtained using a Zeiss LSM 710 Confocal Microscope (Zeiss, Oberkochen, Germany). Stacks were collected using Zen software (Zeiss) and images were processed using Adobe Photoshop CS5 software adjusting only brightness and contrast.

517 **Real-Time PCR of Isolated Taste Cells**

518 Taste receptor cells from CV, Fol or Fun papillae were isolated from the papillae
519 as described above and then centrifuged for 20min at 13,000 RPM. RNA was purified
520 using the NucleoSpin RNA XS Kit (Macherey-Nagel, Düren, Germany) according to kit
521 instructions. PCR analysis was performed for GAPDH to ensure sample quality and
522 check for genomic contamination. Contaminated samples were discarded and new
523 samples were collected. Real-Time PCR was performed using a BioRad MiniOpticon
524 system (Bio-Rad Laboratories, Hercules, CA), with BioRad SYBR Green reagents (Bio-
525 Rad Laboratories). Primers used for these experiments were: **PLCβ2**, *Fwd*:
526 CAATTGAGGGGCAGCTGAGA *Rev*: TTCTAGGCTGCATCTGGGC; **PLCβ3**, *Fwd*:
527 TCCTGGTGGTCAGGGAT *Rev*: CTGCCTGTCTCTGCTATCCG; **GAPDH** *Fwd*:
528 ACAGTCAGCCGCATCTTCTT, *Rev*: ACGACCAAATCCGTTGACTC.

529 For real-time PCR analyses, each sample was run in triplicate. If there was more
530 than 5% difference between the replicates, the data were discarded. Multiple biological
531 repeats were used for each papillae type (CV, n=6; Fol, n=6; Fun, n=5). Data was
532 normalized to GAPDH expression for each sample to correct for any loading differences
533 and reported as fold differences.

534 **Oral Infusions**

535 Wild type, IP_3R3-KO and PLCβ3-KO mice (n=3 for each) were tested to measure
536 the effects of quinine stimulation on the c-Fos immunoreactivity in the nucleus of the
537 solitary tract (NTS). Water infusions (n=3) were performed to measure background
538 responses. Surgical procedures were conducted using sterile technique while mice
539 were anesthetized via 2% - 4% isoflurane anesthesia. Guided by a 21G needle, a small

length of PE-90 tubing was passed through the animal's cheek, emerging into the oral cavity by the rear molars. The tubing was threaded through Teflon washers and heat flared to secure on both the external and oral sides. Mice were given an analgesic (0.5mg/ml of carprofen) and allowed to recover. After recovery, they were infused with either quinine (5mM) or water into the oral catheter for 30 minutes (0.2ml/min, 30 min infusion). Following the infusion, animals were returned to their cages and left undisturbed for 45 minutes.

Brain Histology and Analysis

After the 45 minute post-infusion period, mice were perfused as described above and the hindbrains were removed. The following day, hindbrains were sectioned into 40µm coronal sections which were washed in TBS (pH 7.5), 3x10 min each. Sections were incubated in 1:100 H_2O_2 in TBS for 15 min, followed by 3X10 min TBS washes. Sections were then incubated in anti-c-Fos (ab190289; Abcam, 1:1000) diluted in blocking buffer (3% Normal Donkey Serum in TBS-TritonX) for 1 hr at RT. This was followed by an overnight incubation at 4°C. The next day, sections were washed 3x10 min in TBS and then incubated for 2 hrs in anti-rabbit secondary antibody (711-065-152, Jackson Immunoresearch, 1:1000) in blocking buffer. After incubation, sections were kept in an avidin-biotin mixture (Elite kit; Vector Laboratories) in TBS-TritonX for 1 hr. Tissue sections were washed (3x10 min in TBS) and then stained with DAB (3,3'-diaminobenzidine-HCL; Vector Laboratories) for 5 min. Stained tissue sections were washed (3x5 min in TBS) and mounted onto slides using Fluoromount-G (Southern Biotechnology Associates). Sections were examined using a light microscope (10-100 X) equipped with a digital camera. Analyses of digital images were performed on the

563 intermediate rostral nucleus tractus solitarius (iRNTS; ~500 µm caudal to the dorsal
564 cochlear nucleus) which receives afferents from both the glossopharyngeal and chorda
565 tympani nerves and displays dense c-Fos-like immunoreactivity in response to intraoral
566 delivery of quinine (42, 73). A template tracing of the nucleus was made by an
567 experimenter blind to genotype and stimulus condition and this template was applied to
568 all sections. The number of FLI-positive neurons within the template was counted by
569 hand by an experimenter blind to genotype. Data were analyzed with a one way
570 ANOVA with follow up Student's t tests to identify individual differences. Significance
571 level was set at $p<0.05$.

572 **Analysis of Licking Behavior**

573 Unconditioned licking responses to varying concentrations of taste stimuli were
574 recorded in a test chamber designed to measure brief-access licking (Davis MS80 Rig;
575 Dilog Instruments and Systems, Tallahassee, FL). This apparatus consisted of a
576 Plexiglas cage with a wire mesh floor. An opening at the front of the cage allowed
577 access to one of sixteen spill-proof glass drinking tubes that reside on a sliding platform.
578 A mechanical shutter opened and closed to allow the mouse access to one of the tubes
579 for a user-specified length of time. A computer controlled the movement of the platform,
580 order of tube presentation, opening and closing of the shutter, duration of tube access
581 and interval between tube presentations. Each individual lick was detected by a contact
582 lickometer and recorded on a computer via DavisPro collection software (Dilog
583 Instruments and Systems).

584 Mice were adapted to the test chamber and trained to drink from the sipper tubes
585 for 5 consecutive days as previously described (74, 75). During training, mice were 20-

h water deprived. On the first day of training, the mouse was presented with a single stationary bottle of water for 30 min. On the second day, a tube containing water was presented but this time the mouse was given 180s to initiate licking and once licking was recorded the mouse was given 30s access to the tube. At the conclusion of either the 30s access or the 180s limit, the shutter was closed again for 10s. Each of the 8 tubes, all containing water, was presented 3 times. During the remaining three days of training, the mouse was given 30 min to initiate licking to one of eight tubes of water. Once the mouse began licking, it was given 10s to lick before the shutter closed for 10s, after which a new tube was presented.

During testing, animals were allowed to take as many trials as possible in 30 min. Mice were tested on varying concentrations of sucrose (0,3,10,30,60,100,300,1000 mM), acesulfame K (0,0.5,2,6,8,16,20,32 mM), MSG with 10 μM amiloride (0,25,50,75,100,400,600,800 mM), denatonium benzoate (0,0.1,0.3,1,3,5,10,20 mM), and NaCl (0,3,10,30,60,100,300,1000 mM), in that order. Each stimulus was presented in randomized blocks on Monday, Wednesday and Friday in a single week. Animals were 22-h water deprived for all testing except sucrose, when animals were tested water replete. Once the animal began licking the tube, they were allowed 10 seconds of access before the shutter closed.

For stimuli tested in the water deprived condition (acesulfame K, MSG + amiloride, denatonium benzoate, and NaCl), lick ratios were calculated by dividing the average number of licks at each concentration by the average number of licks to water. For stimuli tested while the animals were water replete (sucrose) licks scores were calculated by subtracting the average number of licks at each concentration by the

609 average number of licks to water. These corrections are used to standardize for
610 individual differences in lick rate and are based on water need. Lick scores and licks
611 relative to water are compared by repeated measures ANOVA with genotype as
612 between factors variable and concentration as a repeated measures within factors
613 variable. Significant interaction terms were followed by Tukey's Honestly Significant
614 Difference tests. Statistical analyses were performed in Statistica.

615 **Solutions**

616 All chemicals were purchased from Sigma Chemical (Sigma-Aldrich, St. Louis,
617 MO) unless otherwise noted. Tyrode's solution contained 140mM NaCl, 5mM KCl, 3mM
618 $CaCl_2$, 1mM $MgCl_2$, 10mM HEPES, 10mM glucose, and 1mM pyruvate, pH 7.4. Ca^{2+}-
619 free Tyrode's contained 140mM NaCl, 5mM KCl, 2.7mM BAPTA, 2mM EGTA, 10mM
620 HEPES, 10mM glucose, 1mM pyruvate, pH 7.4. Nominal Ca^{2+}-free Tyrode's contained
621 140mM NaCl, 5mM KCl, 10mM HEPES, 10mM glucose, 1mM pyruvate, pH 7.4. Hi KCl
622 solution contained 50mM KCl, 90mM NaCl, 3mM $CaCl_2$, 1mM $MgCl_2$, 10mM HEPES,
623 10mM glucose, 1mM pyruvate, pH 7.4. All taste-solutions, 2μM U73122 (Tocris, Bristol,
624 United Kingdom), and 2μM thapsigargin (Tocris) were prepared in normal Tyrode's.
625 Multiple taste stimuli were analyzed for bitter (5mM denatonium benzoate (Den), sweet
626 (20mM sucralose, 2mM saccharin, 50mM sucrose, 20mM Acesulfame K (Ace K)), and
627 umami (10mM monopotassium glutamate (MPG)). 50mM sucrose contained 90mM
628 NaCl instead of 140mM. Salt (250mM sodium chloride, NaCl) and sour (50mM citric
629 acid, CA, pH4) stimuli were tested using the same protocol as Lewandowski et al (19).

630 **Statistics**

631 Analysis of the taste responsiveness was performed using an interactive Chi-
632 square analysis with Yate's correction for continuity (76). Significant differences were
633 reported if $p<0.05$. For real-time PCR analyses, a one-way ANOVA with $p<0.05$ set as
634 the limit of significance was used to identify any significant differences between the
635 relative expression of PLCβ2 and PLCβ3 in the different papillae types. Comparisons
636 between two experimental conditions were made using a two-tailed Student's T test with
637 $p<0.05$ set as the limit of significance.

638 **Colocalization analysis**

639 Image stacks (n=5, 1 μm each) were acquired from labelled sections obtained
640 from three different animals and regions of interest (ROI) were drawn to include the
641 area inside clearly identifiable taste buds. Colocalization analysis was performed on the
642 ROIs using ImageJ Fiji software (NIH). Colocalization was determined based on
643 Pearson's coefficient using the Colocalization_Finder plugin. If the Pearson's coefficient
644 value was greater than 0.9, we considered it to be 100% colocalization due to the
645 variability in immunofluorescence intensity. If the Pearson's coefficient was less than
646 0.05, we considered this to be no colocalization. A Pearson's coefficient higher than
647 0.05 but lower than 0.9 was considered as partial colocalization.

648 **ACKNOWLEDGMENTS**
649 The authors thank Dr. Stefan Roberts at the University of Bristol for comments. This
650 work was supported by NSF1256950 to KFM. The authors thank Alan Siegel and the
651 UB North Campus Imaging facility funded by NSF-MRI DBI0923133 for the confocal
652 images. The authors thank Jhanna Flora for generating our model images.
653

654 **AUTHOR CONTRIBUTIONS**
655 DDB and EDB did live cell imaging, immunohistochemistry, data analysis and
656 contributed to writing the manuscript. DDB also did infusion experiments. LEM
657 performed brief-access lick behavior experiments, infusion experiments and data
658 analysis. KEK performed infusion experiments and data analysis. GCL conceived and

659 analyzed infusion experiments. ARN did immunohistochemistry, qPCR and data
660 analysis. ZCA and BRK did live cell imaging and data analysis. BTK did
661 immunohistochemistry. AV did experiments and analyzed data. AMT supervised brief-
662 access lick behavior, infusion experiments, analyzed and interpreted the data, and
663 edited the manuscript. KFM conceived and supervised the project, did live cell imaging,
664 data analysis and wrote the manuscript.
665
666 The authors declare no competing interests.
667
668

669 **REFERENCES**

670 1. Chaudhari N & Roper SD (2010) The cell biology of taste. *J Cell Biol* 190(3):285-
671 296.
672 2. Finger TE (2005) Cell types and lineages in taste buds. *Chem Senses* 30 Suppl
673 1:i54-55.
674 3. Lawton DM, Furness DN, Lindemann B, & Hackney CM (2000) Localization of
675 the glutamate-aspartate transporter, GLAST, in rat taste buds. *Eur J Neurosci*
676 12(9):3163-3171.
677 4. Miyoshi MA, Abe K, & Emori Y (2001) IP(3) receptor type 3 and PLCbeta2 are
678 co-expressed with taste receptors T1R and T2R in rat taste bud cells. *Chem*
679 *Senses* 26(3):259-265.
680 5. Zhang Y*, et al.* (2003) Coding of sweet, bitter, and umami tastes: different
681 receptor cells sharing similar signaling pathways. *Cell* 112(3):293-301.
682 6. Yan W*, et al.* (2001) Bitter taste transduced by PLC-beta(2)-dependent rise in
683 IP(3) and alpha-gustducin-dependent fall in cyclic nucleotides. *Am J Physiol Cell*
684 *Physiol* 280(4):C742-751.
685 7. Dutta Banik D, Martin LE, Freichel M, Torregrossa AM, & Medler KF (2018)
686 TRPM4 and TRPM5 are both required for normal signaling in taste receptor cells.
687 *Proc Natl Acad Sci U S A* 115(4):E772-E781.
688 8. Taruno A*, et al.* (2013) CALHM1 ion channel mediates purinergic
689 neurotransmission of sweet, bitter and umami tastes. *Nature* 495(7440):223-226.
690 9. Liu D & Liman ER (2003) Intracellular Ca2+ and the phospholipid PIP2 regulate
691 the taste transduction ion channel TRPM5. *Proc Natl Acad Sci U S A*
692 100(25):15160-15165.
693 10. Zhang Z, Zhao Z, Margolskee R, & Liman E (2007) The transduction channel
694 TRPM5 is gated by intracellular calcium in taste cells. *J Neurosci* 27(21):5777-
695 5786.
696 11. Perez CA*, et al.* (2002) A transient receptor potential channel expressed in taste
697 receptor cells. *Nat Neurosci* 5(11):1169-1176.
698 12. Clapp TR, Yang R, Stoick CL, Kinnamon SC, & Kinnamon JC (2004)
699 Morphologic characterization of rat taste receptor cells that express components
700 of the phospholipase C signaling pathway. *J Comp Neurol* 468(3):311-321.
701 13. Yee CL, Yang R, Bottger B, Finger TE, & Kinnamon JC (2001) "Type III" cells of
702 rat taste buds: immunohistochemical and ultrastructural studies of neuron-
703 specific enolase, protein gene product 9.5, and serotonin. *J Comp Neurol*
704 440(1):97-108.
705 14. Simon SA, de Araujo IE, Gutierrez R, & Nicolelis MA (2006) The neural
706 mechanisms of gustation: a distributed processing code. *Nat Rev Neurosci*
707 7(11):890-901.
708 15. Roper SD (2007) Signal transduction and information processing in mammalian
709 taste buds. *Pflugers Arch* 454(5):759-776.
710 16. Clapp TR, Medler KF, Damak S, Margolskee RF, & Kinnamon SC (2006) Mouse
711 taste cells with G protein-coupled taste receptors lack voltage-gated calcium
712 channels and SNAP-25. *BMC Biol* 4:7.

17. Chang RB, Waters H, & Liman ER (2010) A proton current drives action potentials in genetically identified sour taste cells. *Proc Natl Acad Sci U S A* 107(51):22320-22325.
18. Ye W*, et al.* (2016) The K+ channel KIR2.1 functions in tandem with proton influx to mediate sour taste transduction. *Proc Natl Acad Sci U S A* 113(2):E229-238.
19. Lewandowski BC, Sukumaran SK, Margolskee RF, & Bachmanov AA (2016) Amiloride-Insensitive Salt Taste Is Mediated by Two Populations of Type III Taste Cells with Distinct Transduction Mechanisms. *J Neurosci* 36(6):1942-1953.
20. Huang YA, Maruyama Y, Stimac R, & Roper SD (2008) Presynaptic (Type III) cells in mouse taste buds sense sour (acid) taste. *J Physiol* 586(12):2903-2912.
21. Huang AL*, et al.* (2006) The cells and logic for mammalian sour taste detection. *Nature* 442(7105):934-938.
22. Kataoka S*, et al.* (2008) The candidate sour taste receptor, PKD2L1, is expressed by type III taste cells in the mouse. *Chem Senses* 33(3):243-254.
23. Oka Y, Butnaru M, von Buchholtz L, Ryba NJ, & Zuker CS (2013) High salt recruits aversive taste pathways. *Nature* 494(7438):472-475.
24. Damak S*, et al.* (2006) Trpm5 null mice respond to bitter, sweet, and umami compounds. *Chem Senses* 31(3):253-264.
25. Hisatsune C*, et al.* (2007) Abnormal Taste Perception in Mice Lacking the Type 3 Inositol 1,4,5-Trisphosphate Receptor. *J Biol Chem* 282(51):37225-37231.
26. Damak S*, et al.* (2003) Detection of sweet and umami taste in the absence of taste receptor T1r3. *Science* 301(5634):850-853.
27. Danilova V, Damak S, Margolskee RF, & Hellekant G (2006) Taste responses to sweet stimuli in alpha-gustducin knockout and wild-type mice. *Chem Senses* 31(6):573-580.
28. Dotson CD, Roper SD, & Spector AC (2005) PLCbeta2-independent behavioral avoidance of prototypical bitter-tasting ligands. *Chem Senses* 30(7):593-600.
29. Matsumoto I, Ohmoto M, Narukawa M, Yoshihara Y, & Abe K (2011) Skn-1a (Pou2f3) specifies taste receptor cell lineage. *Nat Neurosci* 14(6):685-687.
30. Yee KK, Sukumaran SK, Kotha R, Gilbertson TA, & Margolskee RF (2011) Glucose transporters and ATP-gated K+ (KATP) metabolic sensors are present in type 1 taste receptor 3 (T1r3)-expressing taste cells. *Proc Natl Acad Sci U S A* 108(13):5431-5436.
31. Maruyama Y, Pereira E, Margolskee RF, Chaudhari N, & Roper SD (2006) Umami responses in mouse taste cells indicate more than one receptor. *J Neurosci* 26(8):2227-2234.
32. Hacker K, Laskowski A, Feng L, Restrepo D, & Medler K (2008) Evidence for two populations of bitter responsive taste cells in mice. *J Neurophysiol* 99(3):1503-1514.
33. Clapp TR, Stone LM, Margolskee RF, & Kinnamon SC (2001) Immunocytochemical evidence for co-expression of Type III IP3 receptor with signaling components of bitter taste transduction. *BMC Neurosci* 2:6.
34. DeFazio RA*, et al.* (2006) Separate populations of receptor cells and presynaptic cells in mouse taste buds. *J Neurosci* 26(15):3971-3980.

35. Shandilya J, Gao Y, Nayak TK, Roberts SG, & Medler KF (2016) AP1 transcription factors are required to maintain the peripheral taste system. *Cell Death Dis* 7(10):e2433.
36. Medler KF, Margolskee RF, & Kinnamon SC (2003) Electrophysiological characterization of voltage-gated currents in defined taste cell types of mice. *J Neurosci* 23(7):2608-2617.
37. Sukumaran SK*, et al.* (2017) Whole transcriptome profiling of taste bud cells. *Scientific reports* 7(1):7595.
38. Richter TA, Caicedo A, & Roper SD (2003) Sour taste stimuli evoke Ca2+ and pH responses in mouse taste cells. *J Physiol* 547(Pt 2):475-483.
39. Courtney E Wilson TF, Sue C Kinnamon (2017) Type III cells in anterior taste fields are more immunohistochemically diverse than those of posterior taste fields in mice. *Chemical Senses* bjx055.
40. Yang R, Crowley HH, Rock ME, & Kinnamon JC (2000) Taste cells with synapses in rat circumvallate papillae display SNAP-25-like immunoreactivity. *J Comp Neurol* 424(2):205-215.
41. King CT, Garcea M, & Spector AC (2000) Glossopharyngeal nerve regeneration is essential for the complete recovery of quinine-stimulated oromotor rejection behaviors and central patterns of neuronal activity in the nucleus of the solitary tract in the rat. *J Neurosci* 20(22):8426-8434.
42. King CT, Travers SP, Rowland NE, Garcea M, & Spector AC (1999) Glossopharyngeal nerve transection eliminates quinine-stimulated fos-like immunoreactivity in the nucleus of the solitary tract: implications for a functional topography of gustatory nerve input in rats. *J Neurosci* 19(8):3107-3121.
43. Stratford JM & Finger TE (2011) Central representation of postingestive chemosensory cues in mice that lack the ability to taste. *J Neurosci* 31(25):9101-9110.
44. Stratford JM & Thompson JA (2016) MSG-Evoked c-Fos Activity in the Nucleus of the Solitary Tract Is Dependent upon Fluid Delivery and Stimulation Parameters. *Chem Senses* 41(3):211-220.
45. Stratford JM, Thompson JA, & Finger TE (2017) Immunocytochemical organization and sour taste activation in the rostral nucleus of the solitary tract of mice. *J Comp Neurol* 525(2):271-290.
46. Ruiz-Avila L, Wong GT, Damak S, & Margolskee RF (2001) Dominant loss of responsiveness to sweet and bitter compounds caused by a single mutation in alpha -gustducin. *Proc Natl Acad Sci U S A* 98(15):8868-8873.
47. Zukerman S, Glendinning JI, Margolskee RF, & Sclafani A (2009) T1R3 taste receptor is critical for sucrose but not Polycose taste. *Am J Physiol Regul Integr Comp Physiol* 296(4):R866-876.
48. Treesukosol Y, Smith KR, & Spector AC (2011) Behavioral evidence for a glucose polymer taste receptor that is independent of the T1R2+3 heterodimer in a mouse model. *J Neurosci* 31(38):13527-13534.
49. Treesukosol Y & Spector AC (2012) Orosensory detection of sucrose, maltose, and glucose is severely impaired in mice lacking T1R2 or T1R3, but Polycose sensitivity remains relatively normal. *Am J Physiol Regul Integr Comp Physiol* 303(2):R218-235.

50. Dvoryanchikov G*, et al.* (2017) Transcriptomes and neurotransmitter profiles of classes of gustatory and somatosensory neurons in the geniculate ganglion. *Nat Commun* 8(1):760.
51. Treesukosol Y, Blonde GD, & Spector AC (2009) T1R2 and T1R3 subunits are individually unnecessary for normal affective licking responses to Polycose: implications for saccharide taste receptors in mice. *Am J Physiol Regul Integr Comp Physiol* 296(4):R855-865.
52. Chaudhari N, Landin AM, & Roper SD (2000) A metabotropic glutamate receptor variant functions as a taste receptor. *Nat Neurosci* 3(2):113-119.
53. Chaudhari N, Maruyama Y, Roper S, & Trubey K (2005) Multiple pathways for signaling glutamate taste in rodents. *Chem Senses* 30 Suppl 1:i29-i30.
54. Chaudhari N, Pereira E, & Roper SD (2009) Taste receptors for umami: the case for multiple receptors. *Am J Clin Nutr* 90(3):738S-742S.
55. Delay ER, Hernandez NP, Bromley K, & Margolskee RF (2006) Sucrose and monosodium glutamate taste thresholds and discrimination ability of T1R3 knockout mice. *Chem Senses* 31(4):351-357.
56. Eddy MC, Eschle BK, & Delay ER (2017) Comparison of the Tastes of L-Alanine and Monosodium Glutamate in C57BL/6J Wild Type and T1r3 Knockout Mice. *Chem Senses* 42(7):563-573.
57. Pal Choudhuri S, Delay RJ, & Delay ER (2015) L-Amino Acids Elicit Diverse Response Patterns in Taste Sensory Cells: A Role for Multiple Receptors. *PLoS One* 10(6):e0130088.
58. Pal Choudhuri S, Delay RJ, & Delay ER (2016) Metabotropic glutamate receptors are involved in the detection of IMP and L-amino acids by mouse taste sensory cells. *Neuroscience* 316:94-108.
59. Stone LM, Barrows J, Finger TE, & Kinnamon SC (2007) Expression of T1Rs and gustducin in palatal taste buds of mice. *Chem Senses* 32(3):255-262.
60. Tomchik SM, Berg S, Kim JW, Chaudhari N, & Roper SD (2007) Breadth of tuning and taste coding in mammalian taste buds. *J Neurosci* 27(40):10840-10848.
61. Gilbertson TA, Boughter JD, Jr., Zhang H, & Smith DV (2001) Distribution of gustatory sensitivities in rat taste cells: whole-cell responses to apical chemical stimulation. *J Neurosci* 21(13):4931-4941.
62. Caicedo A, Kim KN, & Roper SD (2002) Individual mouse taste cells respond to multiple chemical stimuli. *J Physiol* 544(Pt 2):501-509.
63. Hegg CC, Jia C, Chick WS, Restrepo D, & Hansen A (2010) Microvillous cells expressing IP3 receptor type 3 in the olfactory epithelium of mice. *Eur J Neurosci* 32(10):1632-1645.
64. Han SK, Mancino V, & Simon MI (2006) Phospholipase Cbeta 3 mediates the scratching response activated by the histamine H1 receptor on C-fiber nociceptive neurons. *Neuron* 52(4):691-703.
65. Xie W*, et al.* (1999) Genetic alteration of phospholipase C beta3 expression modulates behavioral and cellular responses to mu opioids. *Proc Natl Acad Sci U S A* 96(18):10385-10390.

847 66. Hacker K & Medler KF (2008) Mitochondrial calcium buffering contributes to the
848 maintenance of Basal calcium levels in mouse taste cells. *J Neurophysiol*
849 100(4):2177-2191.
850 67. Laskowski AI & Medler KF (2009) Sodium-calcium exchangers contribute to the
851 regulation of cytosolic calcium levels in mouse taste cells. *J Physiol* 587(Pt
852 16):4077-4089.
853 68. Maliphol AB, Garth DJ, & Medler KF (2013) Diet-induced obesity reduces the
854 responsiveness of the peripheral taste receptor cells. *PLoS One* 8(11):e79403.
855 69. Rebello MR, Maliphol AB, & Medler KF (2013) Ryanodine Receptors Selectively
856 Interact with L Type Calcium Channels in Mouse Taste Cells. *PLoS One*
857 8(6):e68174.
858 70. Rebello MR & Medler KF (2010) Ryanodine receptors selectively contribute to
859 the formation of taste-evoked calcium signals in mouse taste cells. *Eur J*
860 *Neurosci* 32(11):1825-1835.
861 71. Szebenyi SA, Laskowski AI, & Medler KF (2010) Sodium/calcium exchangers
862 selectively regulate calcium signaling in mouse taste receptor cells. *J*
863 *Neurophysiol* 104(1):529-538.
864 72. Bartel DL, Sullivan SL, Lavoie EG, Sevigny J, & Finger TE (2006) Nucleoside
865 triphosphate diphosphohydrolase-2 is the ecto-ATPase of type I cells in taste
866 buds. *J Comp Neurol* 497(1):1-12.
867 73. Harrer MI & Travers SP (1996) Topographic organization of Fos-like
868 immunoreactivity in the rostral nucleus of the solitary tract evoked by gustatory
869 stimulation with sucrose and quinine. *Brain Res* 711(1-2):125-137.
870 74. Martin LE*, et al.* (2017) Salivary proteins alter taste-guided behaviors and taste
871 nerve signaling in rat. *Physiol Behav* 184:150-161.
872 75. Torregrossa AM*, et al.* (2014) Induction of salivary proteins modifies measures of
873 both orosensory and postingestive feedback during exposure to a tannic acid
874 diet. *PLoS One* 9(8):e105232.
875 76. Preacher KJ (2001) Calculation for the chi-square test: An interactive calculation
876 tool for chi-square tests of goodness of fit and independence [Computer
877 software]. . p Available from http://quantpsy.org.
878

879 **FIGURE LEGENDS**

880 **Figure 1. Current taste cell models and experimental setup.** A) Current models of
881 the signal transduction pathways in Type II cells (left) that respond to bitter, sweet, and
882 umami stimuli as well as Type III cells (right) that respond to sour and salty stimuli. B)
883 Example of an isolated taste cell that was stimulated with MPG (10mM) and KCl
884 (50mM). The DIC image is shown first, followed by image of Fura 2-AM loading. The
885 next three images show the ratio (340/380) at different time points as the cell is
886 stimulated. The corresponding calcium (Ca^{2+}) changes are shown in 1C.

887

888 **Figure 2. Loss of IP_3R3 causes a reduction, but not abolishment, of taste cell**
889 **sensitivity to different taste stimuli.** Chi square analysis with Yate's correction for
890 continuity was used to compare the frequency of evoked Ca^{2+} responses to different
891 taste stimuli between wild type (WT) and IP_3R3-KO (KO) mice. A) Table of the mouse
892 line, number of mice tested, number of cells tested and number of responses recorded.
893 The P value for each comparison between WT and IP_3R3-GFP-KO is shown as well as
894 the percent response value. These data include all cells from IP_3R3-GFP-KO mice,
895 both GFP+ and GFP-. B) Graph shows the percentage of overall responsiveness to
896 stimuli for taste cells from the CV, Fol and Fun papillae in WT and IP_3R3-KO. The
897 responsiveness to multiple stimuli was evaluated and is shown for CV (C), FOL (D) and
898 FUN (E), Specific numbers and P values for each are shown in Figure S3. (*, $p<0.05$; **,
899 $p<0.01$; ***, $p<0.001$).

900

Figure 3. Taste-evoked Ca^{2+} release in IP_3R3-KO mice is dependent upon PLC activity and Ca^{2+} release from internal stores. Open columns represent the time that the taste stimulus is presented. The application of Ca^{2+} free Tyrode's is indicated by the dashed lines. The stimulus presented during this time is also in Ca^{2+} free Tyrode's. The gray hatched columns represent the application of either thapsigargin or U73122, both of which are irreversible inhibitors. A) Bitter-evoked taste responses (5mM Den) persist in the absence of extracellular calcium (Ca^{2+}-free) and are abolished by the SERCA pump inhibitor thapsigargin (B) as well as the PLC blocker U73122 (C). D) Responses to sweet stimuli (20mM sucrose) persist in Ca^{2+}-free and are abolished by thapsigargin (E) and U73122 (F). G) Umami stimuli (10mM MPG) persist in Ca^{2+}-free and were abolished by thapsigargin (H) and U73122 (I). Individual data points are shown in Figure S4.

Figure 4. Expression of PLCβ3 in taste cells. Laser scanning confocal micrographs (LSCMs, stack of 5 slices, 1μm each) of PLCβ3 immunostaining in the IP_3R3-KO-GFP mice reveals that PLCβ3 is expressed in a separate population from the GFP positive taste cells in the CV (A, n=5), Fol (B, n=3) and Fun papillae (C, n=4). Scale bar=20μM. D) Co-localization analysis is shown.

Figure 5. Some Type III cells respond to bitter, sweet and umami stimuli. A-C) Representative traces of taste cells that responded to bitter, sweet and/or umami stimuli and Hi KCl (50mM) depolarization with Ca^{2+} signals. Some cells responded to 1 stimulus while others responded to multiple stimuli. D) Representative trace of taste

924 cells from IP_3R3-KO mice that responded to 50mM citric acid (CA), 50mM KCl, bitter
925 (5mM denatonium), sweet (20mM sucralose) and umami (10mM monopotassium
926 glutamate, MPG) stimuli. E) Representative trace of a separate subset of cells that
927 responded to 250mM NaCl, 50mM citric acid (CA) and 50mM KCl but were not sensitive
928 to the bitter, sweet, umami stimuli tested. F) Summary of taste cells from IP_3R3-KO
929 mice that responded to 50mM KCl with a Ca^{2+} signal (n=20), 25% only responded to
930 CA, 35% responded to CA and NaCl, and 40% responded to CA and bitter, sweet
931 and/or umami stimuli (B,U,S) while no cells responded to all the taste stimuli. G) The
932 overall responsiveness of taste cells from the CV, Fol and Fun papillae of the IP_3R3-KO
933 mice and WT mice was measured. This is defined as the percentage of stimulated cells
934 that responded to at least one stimulus. The percentage of DR cells in both lines was
935 also measured using the criteria that the cell responded to at least one stimulus AND
936 50mM KCl with Ca^{2+} signals. The overall responsiveness to taste stimuli was
937 significantly reduced in the IP_3R3-KO mice compared to controls (**,$p<0.01$) while the
938 number of responsive DR cells did not change in the absence of IP_3R3. H) The
939 percentage of responsiveness in the DR taste cells to different taste stimuli in the WT
940 and IP_3R3-KO mice. Chi-square analysis found no significant differences.
941
942 **Figure 6. PLCβ3 is required for the detection of bitter, sweet and umami stimuli.**
943 Chi square analysis with Yate's correction for continuity was used to compare the
944 frequency of evoked Ca^{2+} responses to different taste stimuli between wild type (WT)
945 and PLCβ3-KO (KO) mice. A) Table of the mouse line, number of mice tested, number
946 of cells tested and number of responses recorded. The P value for each comparison

947 between WT and PLCβ3-KO is shown as well as the percent response value. B) The
948 overall responsiveness and the percentage of DR taste cells from the CV, Fol and Fun
949 papillae of the PLCβ3-KO mice and WT mice was measured. Both the overall
950 responsiveness to taste stimuli and the number of DR cells were significantly reduced in
951 the PLCβ3-KO mice compared to controls. The responsiveness to multiple stimuli was
952 evaluated and is shown for CV (C), FOL (D) and FUN (E). Specific numbers and P
953 values for each are shown in Figure S8. (*, $p<0.05$; **, $p<0.01$; ***, $p<0.001$).
954
955 **Figure 7. Loss of PLCβ3 or IP_3R3 causes deficits in the taste-evoked neural**
956 **activity in the nucleus of solitary tract.**
957 Oral infusion of bitter (quinine) and water elicited c-Fos immunoreactivity in the
958 intermediate rostral nucleus tractus solitarius (IRNTS). (A, B) Loss of either PLCβ3
959 (PLCβ3-KO) or IP_3R3 (IP_3R3-KO) caused a significant reduction in the c-Fos
960 immunoreactivity in the IRNTS compared to WT mice. The residual c-Fos labeling in
961 each of the KO mice was comparable to the c-Fos labelling generated by water infusion.
962 For all experiments, 3 mice of each genotype were used (***, $p<0.001$; **, $p<0.01$). The
963 red outlined area denotes the analyzed region for each. Data were analyzed with a one
964 way ANOVA with follow up Student's t tests to identify individual differences.
965 Significance level was set at $p<0.05$. C) A schematic diagram showing the analysis
966 region in the hindbrain that was analyzed.
967
968 **Figure 8. Loss of PLCβ3 or IP_3R3 affects behavioral responses to taste stimuli.**
969 Lick data (±standard deviation) from brief-access behavioral tests compare the

970 responses of IP_3R3-KO (red line) and PLCβ3-KO (pink line) to WT (IP_3R3-WT, black
971 line; PLCβ3-WT, blue line). A) Lick ratios (stimulus/water) of the WT mice for the bitter
972 stimulus denatonium (0, 0.1, 0.3, 1, 3, 5, 10, 20mM) were significantly different from the
973 IP_3R3-KO and PLCβ3-KO responses. B) Lick ratios of the WT mice for the umami
974 stimulus monosodium glutamate + 10μM amiloride (MSG, 0, 25, 50, 75, 100, 400, 600,
975 800mM) were significantly different from the IP_3R3-KO and PLCβ3-KO mice. C) Lick
976 ratios of the WT mice for the artificial sweetener acesulfame K (0, 0.5, 2, 6, 8, 16, 20,
977 32mM) were significantly different from the IP_3R3-KO and PLCβ3-KO mice. D) Lick
978 scores (stimulus-water) of the WT mice for sucrose (0, 3, 10, 30, 60,100, 300, 1000mM)
979 were significantly different from the IP_3R3-KO and PLCβ3-KO responses. E) No
980 significant differences were detected between the WT and KO mice for any
981 concentration of NaCl (0, 3, 10, 30, 60, 100, 300, 1000mM) tested. For all experiments,
982 5 mice of each genotype were used (***, $p<0.001$; **, $p<0.01$; *, $p<0.05$). Data were
983 compared by repeated measures ANOVA. Significant interaction terms were followed
984 by Tukey's Honestly Significant Difference tests.
985

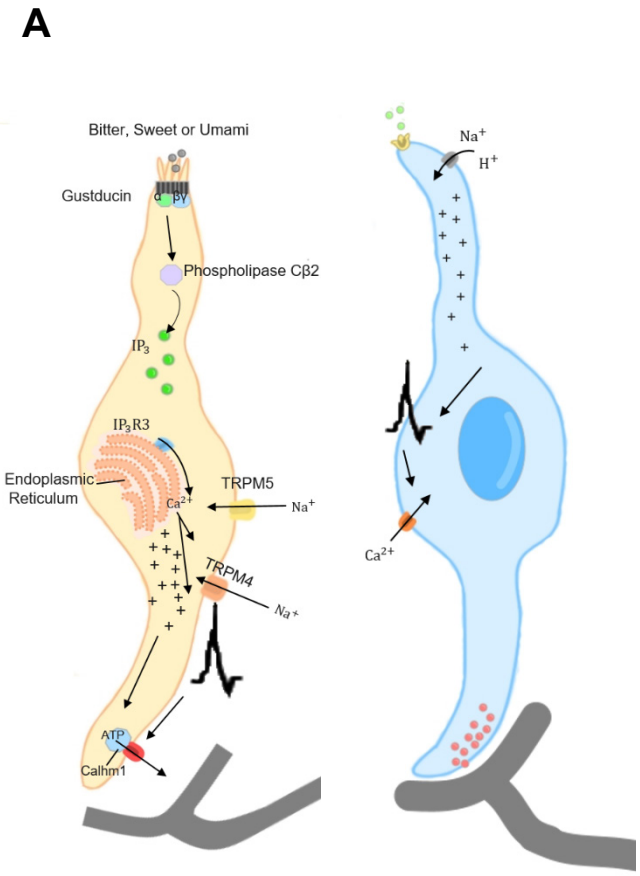
A
Bitter, Sweet or Umami
Gustducin
Phospholipase Cβ2
IP3
IP3R3
Endoplasmic Reticulum
TRPM5
Na+
Ca2+
TRPM4
ATP
Calhm1
Na+
H+
Ca2+

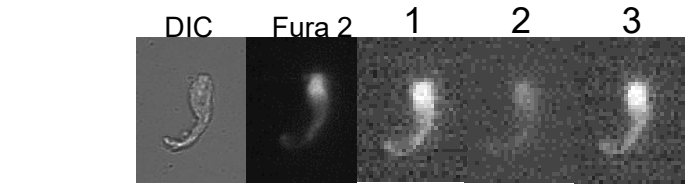
B
DIC
Fura 2
1
2
3

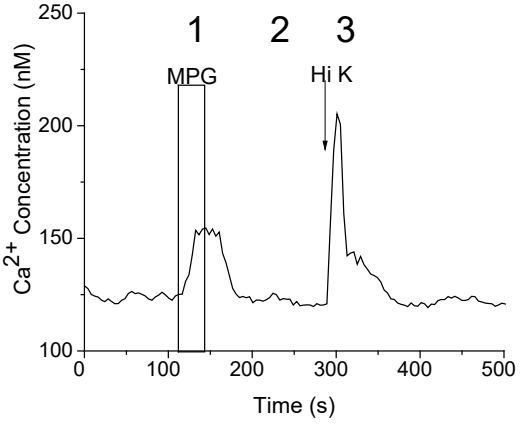
C
1
2
3
MPG
Hi K
Ca2+ Concentration (nM)
250
200
150
100
0
100
200
300
400
500
Time (s)

FIGURE 1

A

Papillae type	Mouse genotype	Cells tested	# of Resp.	P value	% value
All cells	WT (n=105 mice)	407	259	P<0.0001	63.6
	KO (n=115 mice)	690	213		30.9
CV	WT (n=63 mice)	250	159	P=0.0003	63.6
	KO (n=70 mice)	443	172		38.8
FOL	WT (n=28 mice)	53	29	P=0.44	54.7
	KO (n=37 mice)	123	52		42.3
FUN	WT (n=32 mice)	104	71	P=0.17	68.2
	KO (n=30 mice)	124	61		49.2

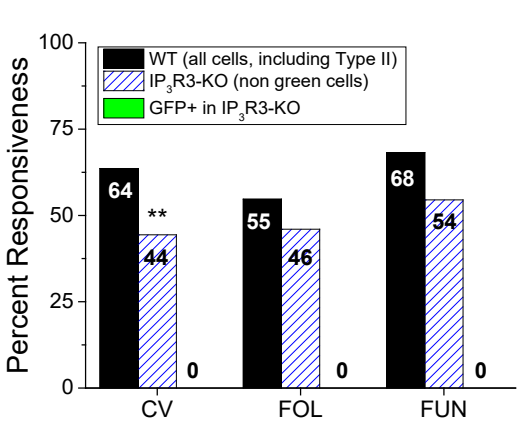

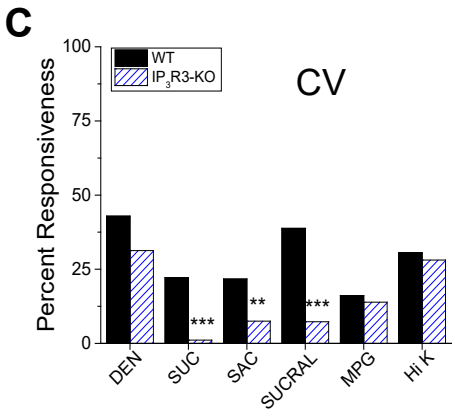

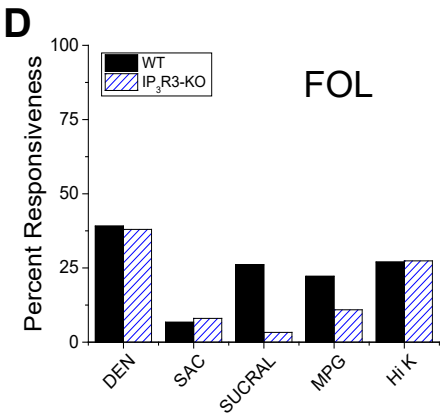

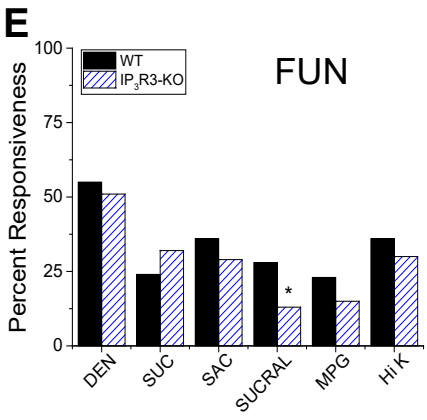

FIGURE 2

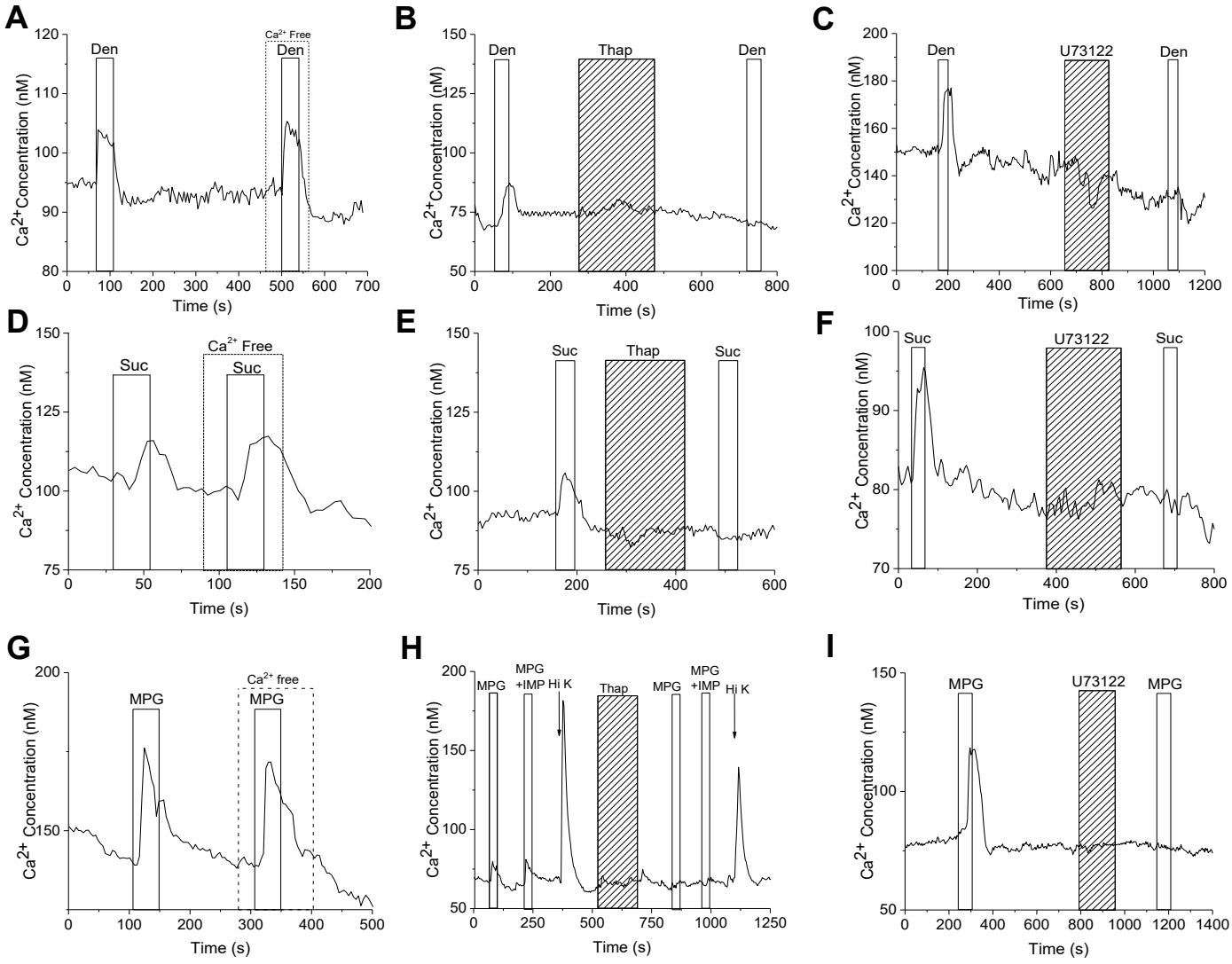
A
Den
Ca2+ Free
Den
Ca2+Concentration (nM)
Time (s)
B
Den
Thap
Den
Ca2+Concentration (nM)
Time (s)
C
Den
U73122
Den
Ca2+Concentration (nM)
Time (s)
D
Suc
Ca2+ Free
Suc
Ca2+ Concentration (nM)
Time (s)
E
Suc
Thap
Suc
Ca2+ Concentration (nM)
Time (s)
F
Suc
U73122
Suc
Ca2+ Concentration (nM)
Time (s)
G
MPG
Ca2+ free
MPG
Ca2+ Concentration (nM)
Time (s)
H
MPG
MPG +IMP
Hi K
Thap
MPG
MPG +IMP
Hi K
Ca2+ Concentration (nM)
Time (s)
I
MPG
U73122
MPG
Ca2+ Concentration (nM)
Time (s)

FIGURE 3

A

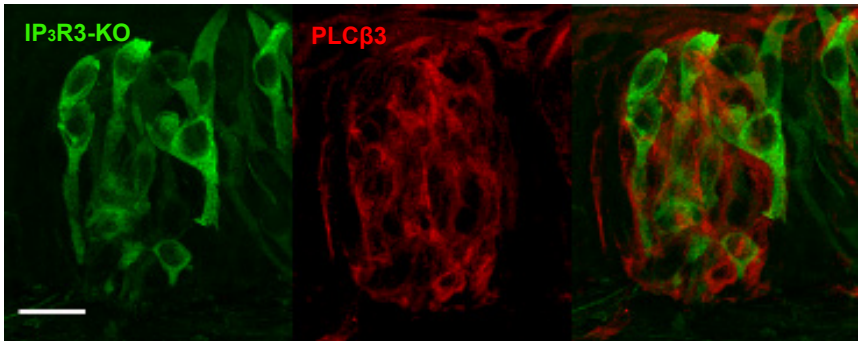

CV

B

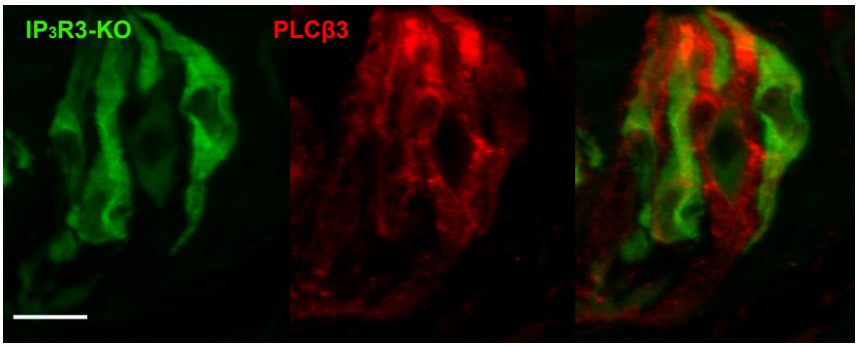

FOL

C

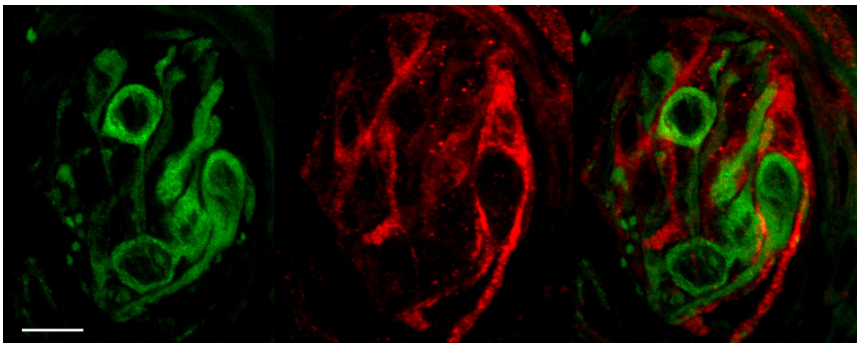

FUN

D

Comparison	Average overlap, standard deviation
GFP vs anti-PLCβ3	0.03±0.02

FIGURE 4

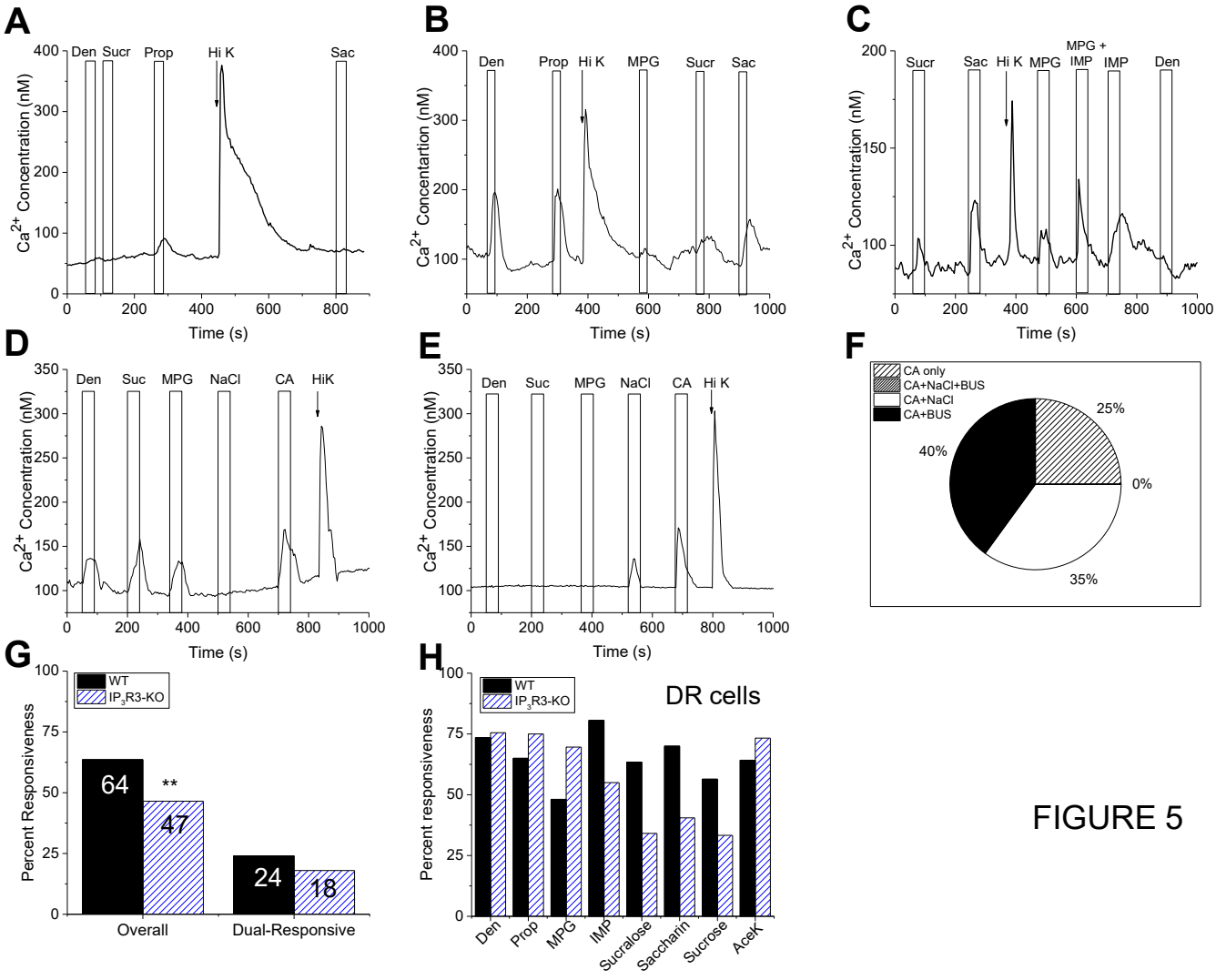
A
Den Sucr Prop Hi K Sac
Ca2+ Concentration (nM)
Time (s)
B
Den Prop Hi K MPG Sucr Sac
Ca2+ Concentration (nM)
Time (s)
C
Sucr Sac Hi K MPG MPG + IMP IMP Den
Ca2+ Concentration (nM)
Time (s)
D
Den Suc MPG NaCl CA HiK
Ca2+ Concentration (nM)
Time (s)
E
Den Suc MPG NaCl CA Hi K
Ca2+ Concentration (nM)
Time (s)
F
CA only
CA+NaCl+BUS
CA+NaCl
CA+BUS
25%
40%
0%
35%
G
WT
IP3R3-KO
Percent Responsiveness
64
**
47
24
18
Overall
Dual-Responsive
H
WT
IP3R3-KO
DR cells
Percent responsiveness
Den
Prop
MPG
IMP
Sucralose
Saccharin
Sucrose
AceK

FIGURE 5

A

Papillae type	Mouse genotype	Cells tested	# of Resp.	P value	% value
All cells	WT (n=53 mice)	577	344	P=0.002	59.6
	KO (n=68 mice)	375	155		41.3
CV	WT (n=40 mice)	221	137	P=0.246	61.9
	KO (n=55 mice)	138	68		49.2
FOL	WT (n=40 mice)	243	136	P=0.039	55.9
	KO (n=34 mice)	120	43		35.8
FUN	WT (n=35 mice)	113	71	P=0.035	62.8
	KO (n=48 mice)	117	44		37.6

B

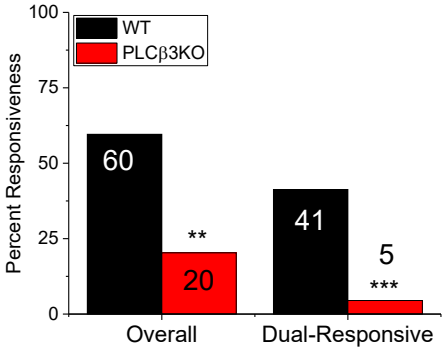

C

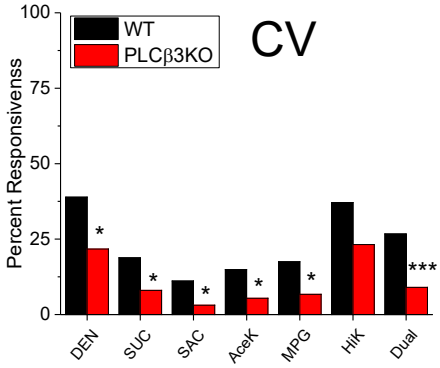

D

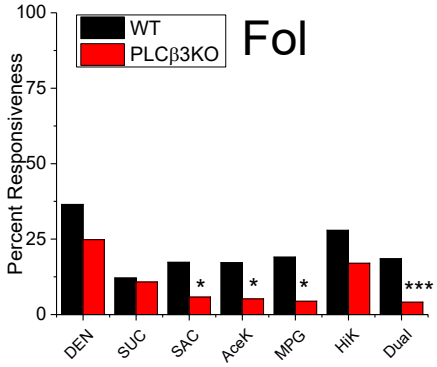

E

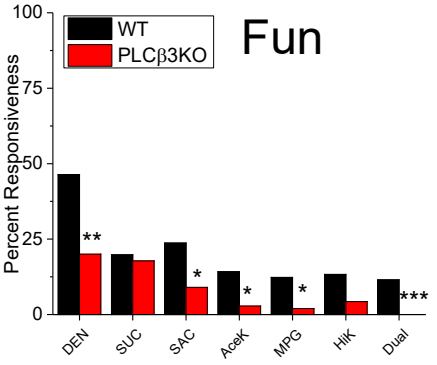

FIGURE 6

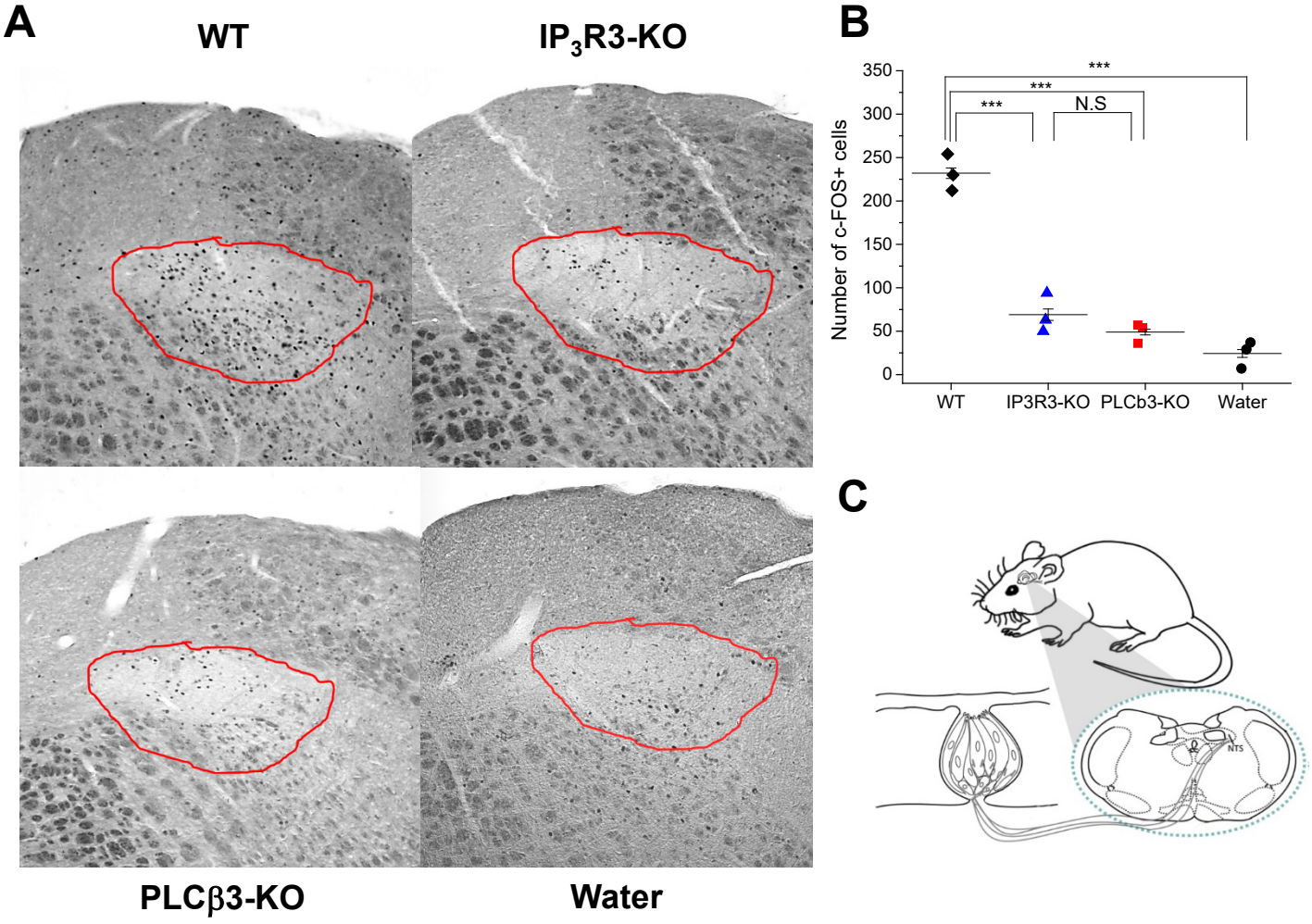
A
WT
IP3R3-KO
PLCβ3-KO
Water
B
Number of c-FOS+ cells
350
300
250
200
150
100
50
0
***
***
***
N.S
WT
IP3R3-KO
PLCb3-KO
Water
C
NTS

FIGURE 7

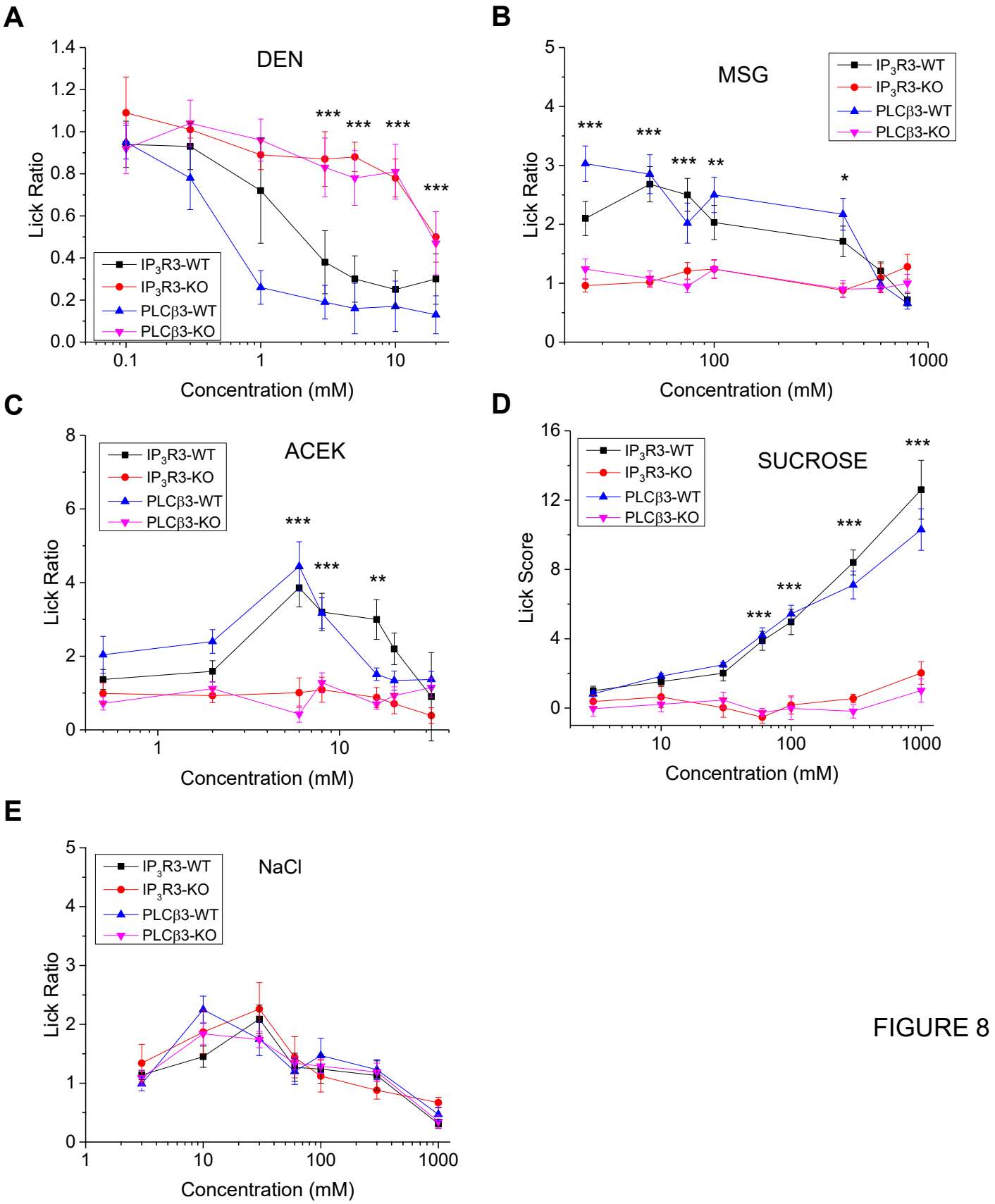
A
DEN
Lick Ratio
Concentration (mM)
IP3R3-WT
IP3R3-KO
PLCβ3-WT
PLCβ3-KO
B
MSG
Lick Ratio
Concentration (mM)
C
ACEK
Lick Ratio
Concentration (mM)
D
SUCROSE
Lick Score
Concentration (mM)
E
NaCl
Lick Ratio
Concentration (mM)

FIGURE 8

Cell populations	**Identifiers/Classification**
IP_3R3-KO-GFP cells	Type II cells with GFP expression replacing IP_3R3 expression.
WT cells	All cells that were tested and/or responded to stimuli, including Type II cells, Type III cells, other cells.
IP_3R3-KO cells	Taste cells from mice that lack functional Type II cells and do not express GFP. These include Type III cells and other cells.
Dual-responsive cells	Taste cells that respond to 50mM KCl (indicating the presence of VGCC) and bitter, sweet and/or umami stimuli.
Taste-only cells	Taste cells from the IP_3R3-KO mouse that lack GFP expression (are not Type II cells) and do not respond to 50mM KCl (are not Type III cells).

Table S1. Definition of taste cell populations analyzed.

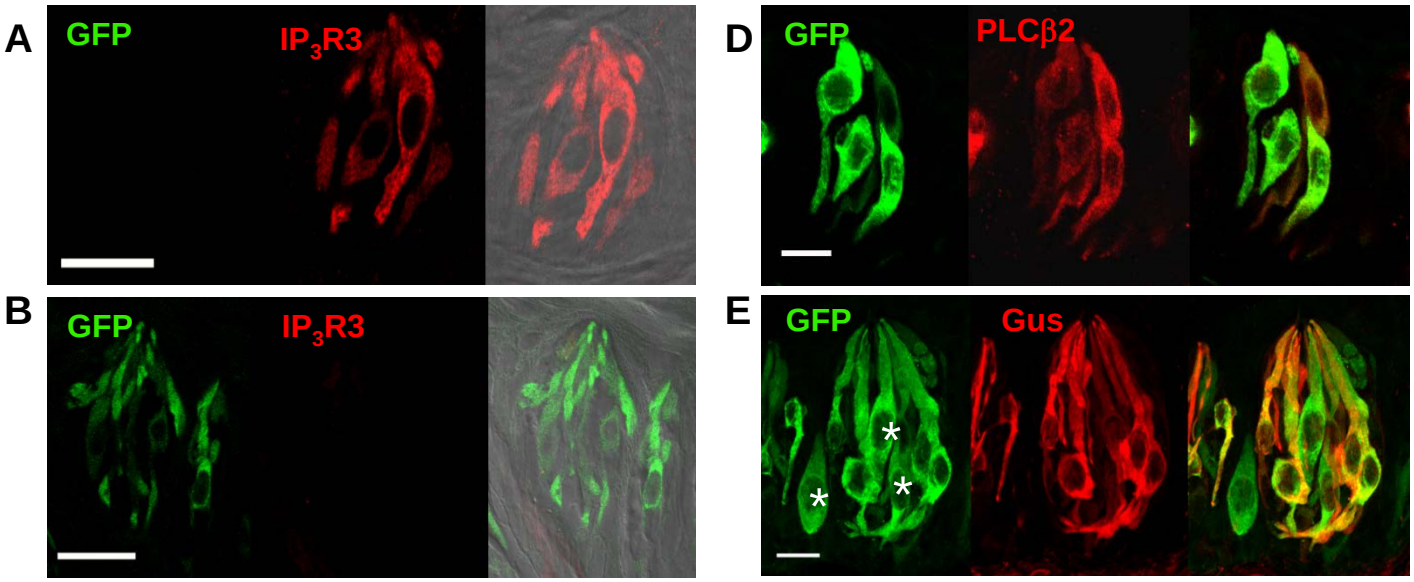

F

Comparison	Average overlap, standard deviation
GFP vs anti-IP_3R3 in het	0.94±0.02
GFP vs anti-PLCβ2	0.97±0.01
GFP vs anti-gustducin	0.31±0.04

Figure S1. Characterization of the IP_3R3-KO mice. A) LSCMs (stack of 5 slices, 1μm each) from WT mice identified anti-IP_3R3 labeling in taste receptor cells from the CV (n=3). B) IP_3R3-KO mice express GFP in lieu of IP_3R3 and were not labeled by anti-IP_3R3 (n=6). C) LSCMs of the IP_3R3-het mouse identified strong co-localization between anti-IP_3R3 labeling and GFP expression. D) Anti-PLCβ2 labeling in IP_3R3-KO mice found that PLCβ2 co-localizes with GFP, indicating that IP_3R3-KO-GFP is specific to Type II cells (LSCMs: stack of 5 slices, 1μm each; n=4). E) α-gustducin is present in a subset of the IP_3R3-KO-GFP taste cells in the CV (LSCMs: stack of 10 slices, 1μm each; n=3). Asterisks identify some GFP expressing cells that do not express gustducin. Scale bars = 20 μm. F) Co-localization analysis identified the average (± standard deviation) overlapping expression for each target protein with the GFP expression, n=3 for each.

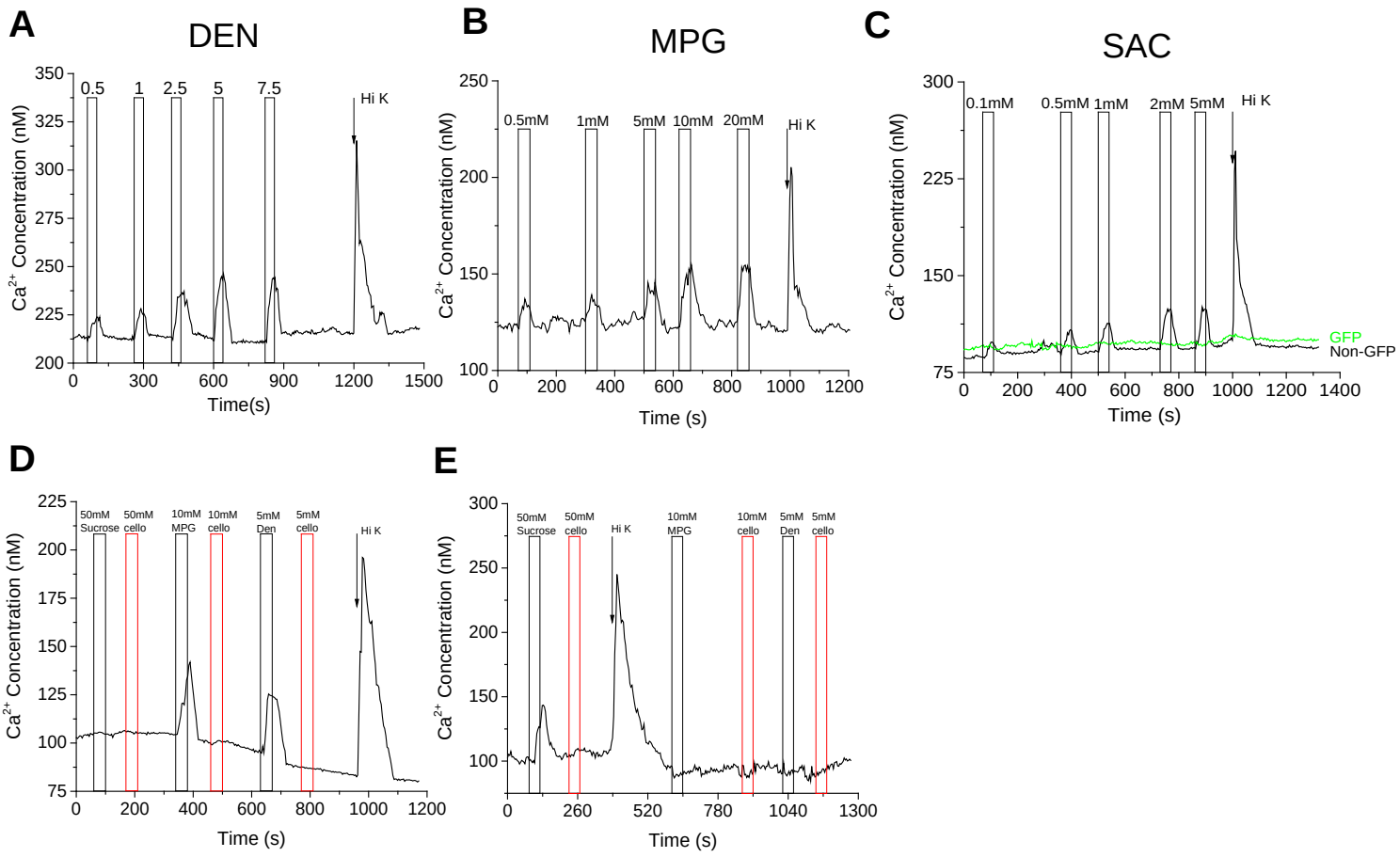

Figure S2. Taste-evoked Ca^{2+} signals are specific to the stimulus.

A concentration gradient analysis of (A) a bitter stimulus (denatonium), (B) an umami stimulus (MPG) and (C) a sweet stimulus (saccharin) demonstrates that DR cells respond to a wide range of stimulus concentrations. The GFP+ cell (lacks IP_3R3) in C did not respond to any concentration of saccharin applied. (D-E) Identical concentrations of the compound cellobiose did not generate a Ca^{2+} signal in DR cells, indicating that the measured responses are taste-activated and not due to non-specific osmotic effects.

IP_3R3

CV

CV Stimulus	MS	Cells tested	# of Resp.	P value
DEN	WT	238	102	0.06
	KO	341	107	
SUC	WT	72	16	0.0004
	KO	87	1	
SAC	WT	106	23	0.005
	KO	174	13	
SUCRAL	WT	121	47	p<0.001
	KO	137	10	
MPG	WT	81	13	0.82
	KO	301	42	
HI K	WT	245	75	0.68
	KO	384	108	

FOL

FOL Stimulus	MS	Cells tested	# of Resp.	P value
DEN	WT	46	18	0.93
	KO	100	38	
SAC	WT	15	1	0.69
	KO	50	4	
SUCRAL	WT	23	6	0.08
	KO	30	1	
MPG	WT	18	4	0.48
	KO	73	8	
HI K	WT	53	14	0.93
	KO	113	31	

FUN

FUN Stimulus	MS	Cells tested	# of Resp.	P value
DEN	WT	76	42	0.89
	KO	59	30	
SUC	WT	41	10	0.89
	KO	19	6	
SAC	WT	65	23	0.73
	KO	55	16	
SUCRAL	WT	85	25	0.04
	KO	99	13	
MPG	WT	75	17	0.4
	KO	81	12	
HI K	WT	104	33	0.7
	KO	103	28	

Figure S3. Tables of the mouse line, number of mice tested, number of cells tested and number of responses recorded from the CV, FOL, and FUN papillae of the WT and IP_3R3-KO mice data shown in Figure 2. Chi-square analysis with Yate's correction for continuity was used to identify significant differences in the response frequency between WT and KO mice for each stimulus in each papillae.

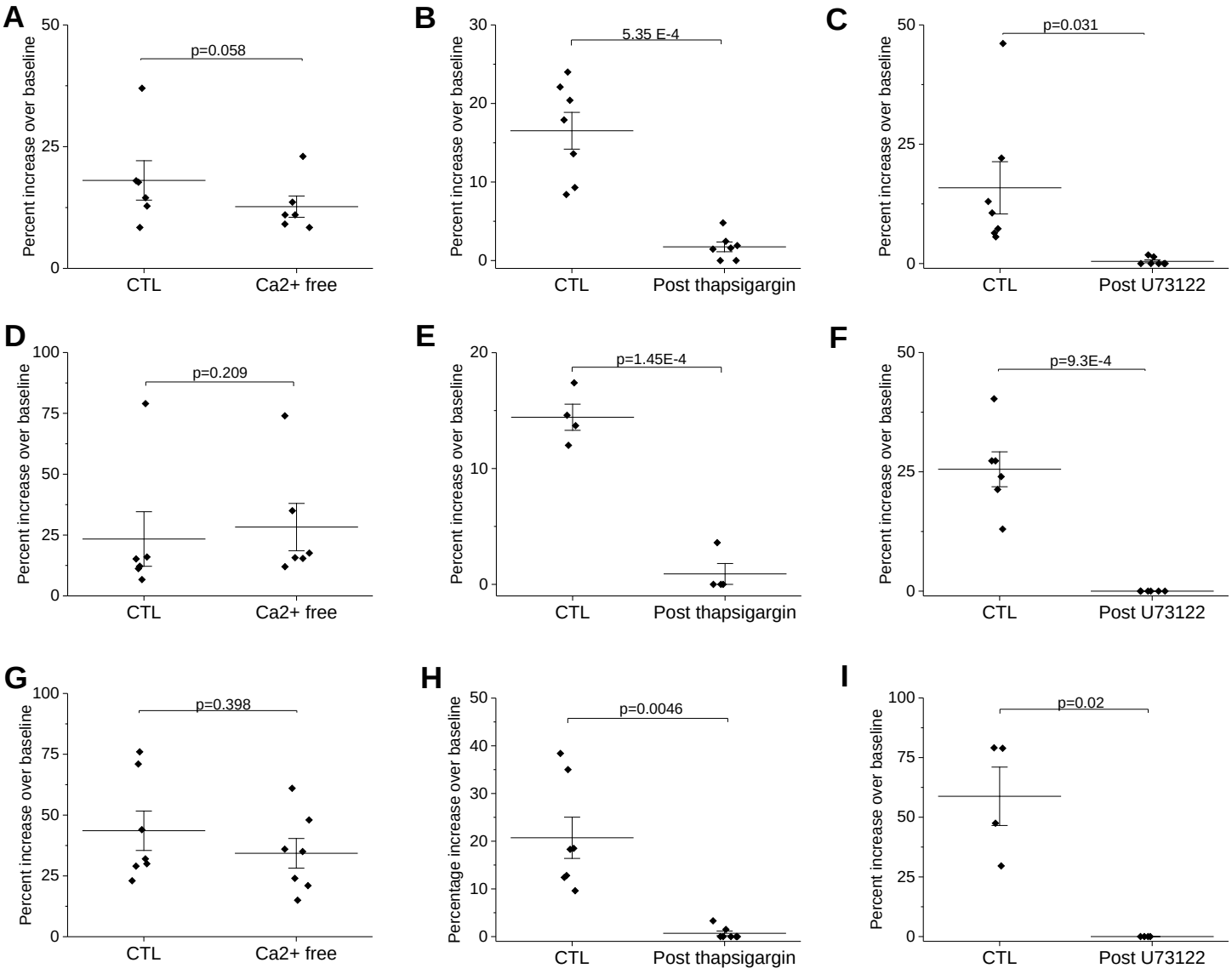

Figure S4. Taste-evoked Ca^{2+} release in IP_3R3-KO mice is dependent upon PLC activity and Ca^{2+} release from internal stores. Individual data points of the data presented in Figure 3. A) Bitter-evoked taste responses (5mM Den, n=6) persist in the absence of extracellular calcium (Ca^{2+}-free) and are abolished by the SERCA pump inhibitor thapsigargin (B, n=7) as well as the PLC blocker U73122 (C, n=7). D) Responses to sweet stimuli (50mM sucrose, n=6) persist in Ca^{2+}-free and are abolished by thapsigargin (E, n=4) and U73122 (F, n=6). G) Umami stimuli (10mM MPG) persist in Ca^{2+}-free (n=7) and were abolished by thapsigargin (H, n=7) and U73122 (I, n=4). A two-tailed Student's t test was used to identify significant differences for each experimental condition.

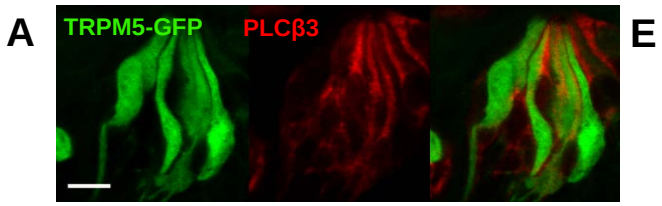

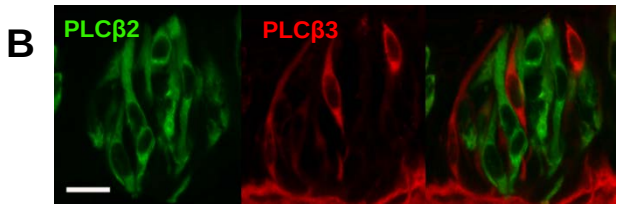

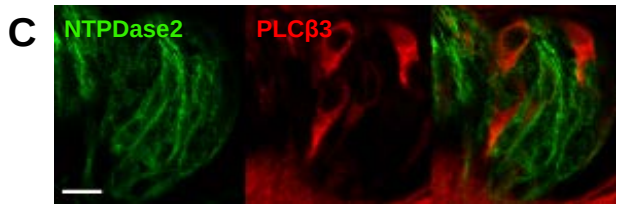

D

Comparison	Average overlap, standard deviation
TRPM5-GFP vs anti-PLCβ3	0.03±0.006
anti-PLCβ2 vs anti-PLCβ3	0.02±0.02

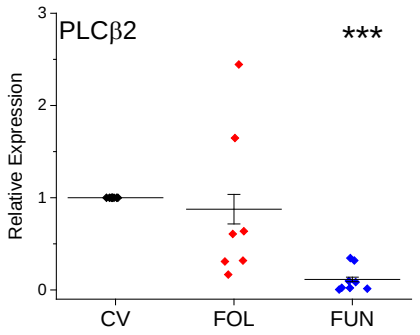

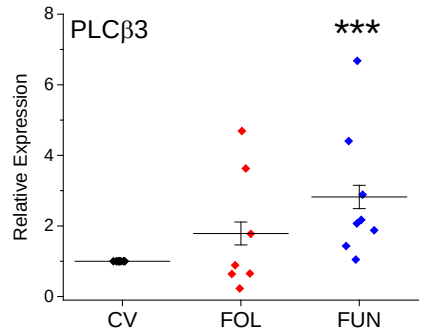

Figure S5. Expression of PLCβ3 in taste papillae. A) Anti-PLCβ3 labeling in the CV of TRPM5-GFP mice determined that PLCβ3 is expressed in taste cells lacking GFP expression (LSCMs: stack of 5 slices, 1μm each; n=4). B) Co-labeling with anti-PLCβ2 and anti-PLCβ3 in the CV of C57BL/6 mice revealed that these PLCβs are expressed in separate taste cell populations (LSCMs: stack of 5 slices, 1μm each; n=3). C) Co-labeling with anti-NTDPase2 and anti-PLCβ3 in the CV of C57BL/6 mice determined that these markers are expressed in separate taste cell populations (LSCMs: stack of 5 slices, 1μm each; n=3). Scale bar = 10μM. D) Co-localization analysis identified the average (± standard deviation) overlapping expression for PLCβ3 with TRPM5-GFP or anti-PLCβ2 expression, n=3 for each. mRNA was isolated from taste cells originating in the different papillae types from C57BL/6 mice. Taste cells were analyzed from at least five different mice for each. Values were normalized to GAPDH expression and are presented as a ratio to values from the CV papillae for (E) PLCβ2 and (F) PLCβ3. (***, $p<0.001$). A one-way ANOVA with $p<0.05$ set as the limit of significance was used to identify any differences in the relative mRNA levels between papillae types.

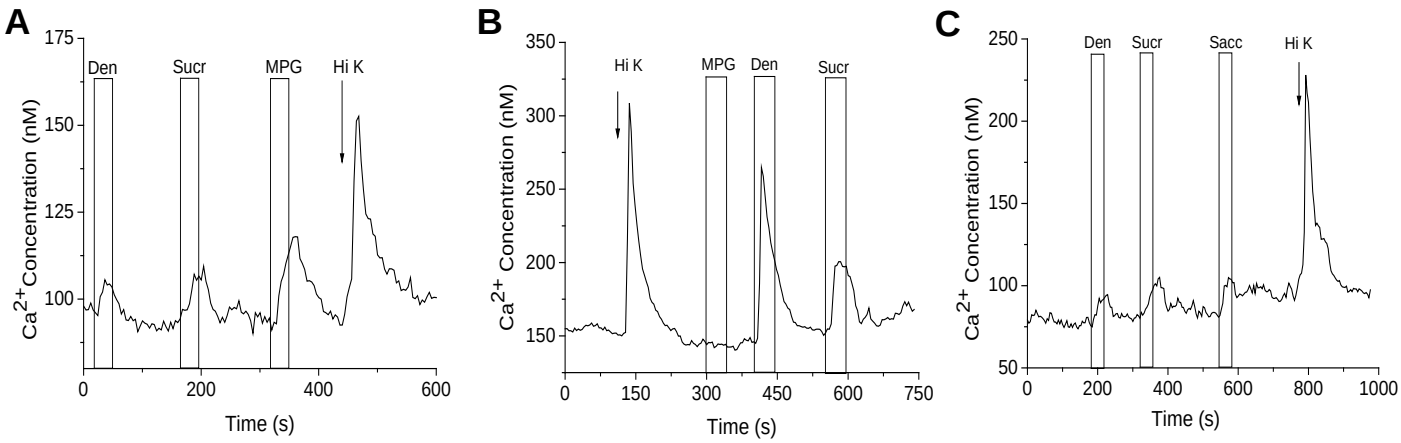

Figure S6. Dual responsive cells are present in multiple mouse lines. Control imaging experiments were performed using GAD67-GFP mice and C57BL/6 mice. GAD67-GFP is expressed in a large subset of Type III mouse taste cells (34). A-B) Representative traces of DR taste cells that responded to bitter, sweet and/or umami stimuli and Hi KCl (50mM) in GAD67-GFP mice. DR taste cells were present in both GAD67-GFP + (A) and -GFP- (B) taste cells. C) Experiments in C57BL/6 mice also identified the presence of DR taste cells.

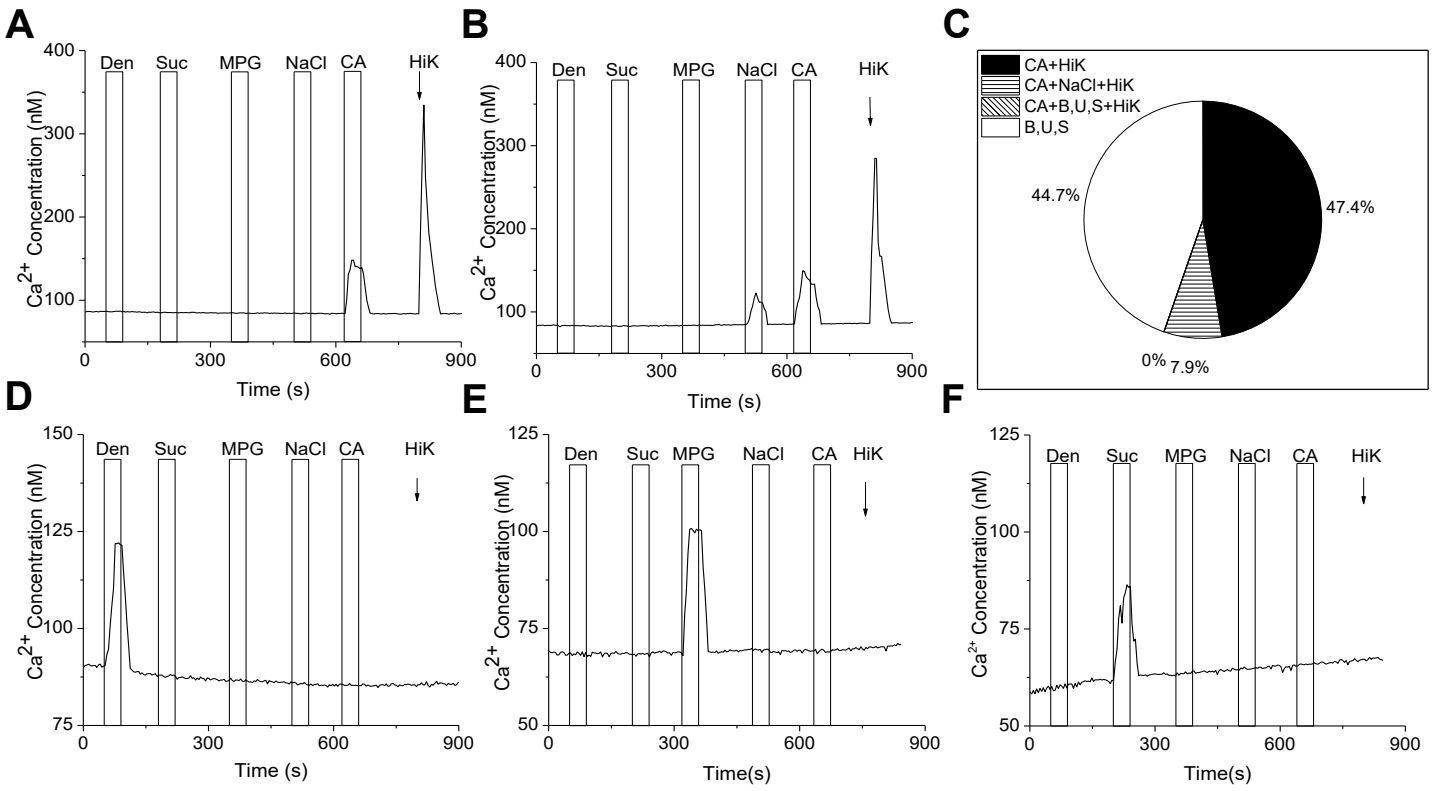

Figure S7. Stimulus evoked Ca^{2+} responses in taste cells in PLCβ3-KO mice. A) Representative trace of taste cells from PLCβ3-KO mice that responded to 50mM citric acid (CA) and KCl (50mM) but did not respond to bitter (5mM denatonium), sweet (20mM sucralose) or umami (10mM monopotassium glutamate, MPG) stimuli. B) Representative trace of a separate subset of cells that responded to 250mM NaCl, CA and KCl but were not sensitive to the bitter, sweet, umami stimuli tested. C) Summary of responsive taste cells from PLCβ3-KO mice (n=38): CA and KCl (n=18); CA, NaCl and KCl (n=3); CA, KCl, and bitter, sweet and/or umami stimuli (B,U,S) (n=0); and B,U,S only (n=17). Representative taste-evoked responses for bitter (D), sweet (E) and umami (F) in the PLCβ3-KO mice. None of these cells responded to CA or KCl.

PLCβ3

CV

CV Stimulus	MS	Cells tested	# of Resp.	P value
DEN	WT	221	86	0.018
	KO	138	30	
SUC	WT	191	36	0.039
	KO	112	9	
SAC	WT	198	22	0.02
	KO	130	4	
ACEK	WT	181	27	0.04
	KO	111	6	
MPG	WT	182	32	0.031
	KO	116	8	
HI K	WT	221	82	0.06
	KO	138	32	
DR	WT	221	59	0.0008
	KO	138	12	

FOL

FOL Stimulus	MS	Cells tested	# of Resp.	P value
DEN	WT	233	85	.144
	KO	113	28	
SUC	WT	173	21	0.97
	KO	65	7	
SAC	WT	156	27	0.04
	KO	86	5	
ACEK	WT	163	28	0.04
	KO	76	4	
MPG	WT	179	34	0.21
	KO	67	3	
HI K	WT	243	68	0.08
	KO	120	20	
DR	WT	243	45	0.002
	KO	120	5	

FUN

FUN Stimulus	MS	Cells tested	# of Resp.	P value
DEN	WT	112	52	0.003
	KO	117	23	
SUC	WT	86	17	0.91
	KO	107	19	
SAC	WT	93	22	0.015
	KO	111	10	
ACEK	WT	84	12	0.015
	KO	108	3	
MPG	WT	81	10	0.016
	KO	107	2	
HI K	WT	113	15	0.053
	KO	116	5	
DR	WT	113	13	0.001
	KO	116	0	

Figure S8. Tables of the mouse line, number of mice tested, number of cells tested and number of responses recorded from the CV, FOL, and FUN papillae of the WT and PLCβ3-KO mice data shown in Figure 6. Chi-square analysis with Yate's correction for continuity was used to identify significant differences in the response frequency between WT and KO mice for each stimulus in each papillae.

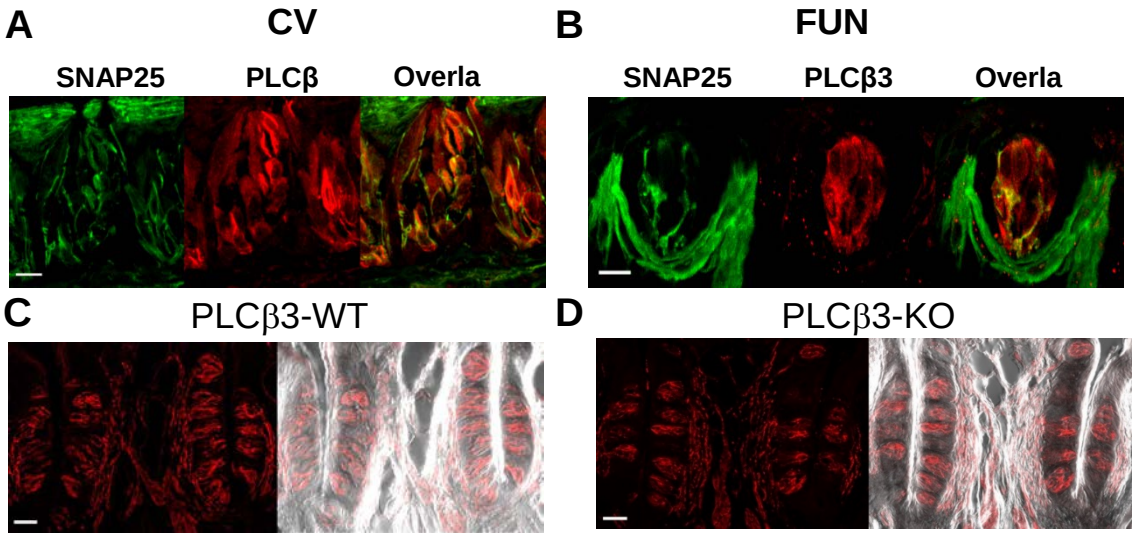

E

Comparison	Average overlap, standard deviation
anti-PLCβ3 vs anti-SNAP25	0.62±0.03

Figure S9. PLCβ3 is expressed in some Type III taste cells. Immunohistochemical analyses (LSCMs: stack of 5 slices, 1μm each) using anti-PLCβ3 and anti-SNAP25 revealed some co-localization between PLCβ3 and SNAP25, confirming that PLCβ3 is expressed in some Type III cells but is not restricted in its expression to this taste cell type (A, CV papillae, n=3; B, Fun papillae, n=3) Scale bar=20μM. Labeling with anti-SNAP25 in the CV of PLCβ3-WT (**C**) and PLCβ3-KO (**D**) mice revealed no differences in the expression level of this synaptic marker (n=5 mice for each). Scale bars = 50 μm. E) Co-localization analysis identified the average (± standard deviation) overlapping expression for PLCβ3 with anti-SNAP25 expression, n=3.

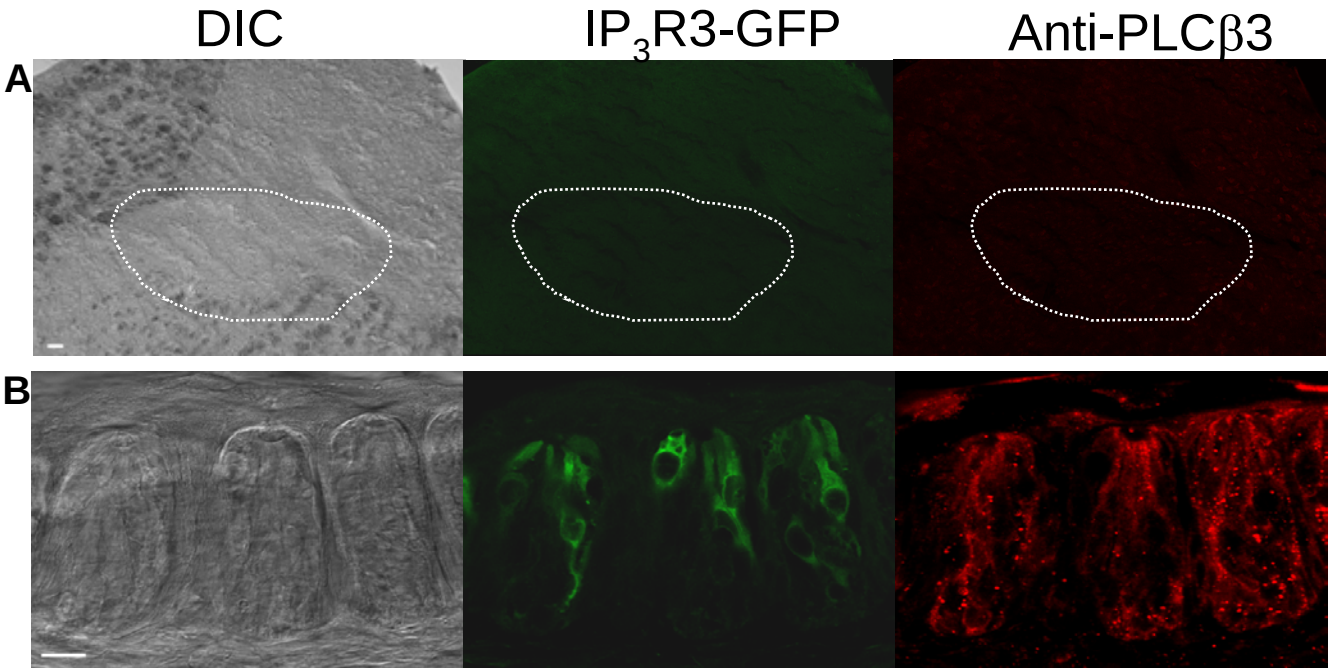

Figure S10. Neither IP_3R3 nor PLCβ3 is expressed in IRNTS.

CV papillae and IRNTS sections were evaluated in parallel. A) Analyses of the brain sections from the IP_3R3-KO mice revealed no GFP labelling in the IRNTS. Immunohistochemical analysis using anti-PLCβ3 also did not detect any PLCβ3 expression. Scale bar=50μm. B) LSCM analyses (n=5 sections, 1 μM each) of the tongues from the same mice identified the expression of IP_3R3-KO-GFP and PLCβ3 in the taste receptor cells from the CV papillae (n=3). Scale bar=10μm.

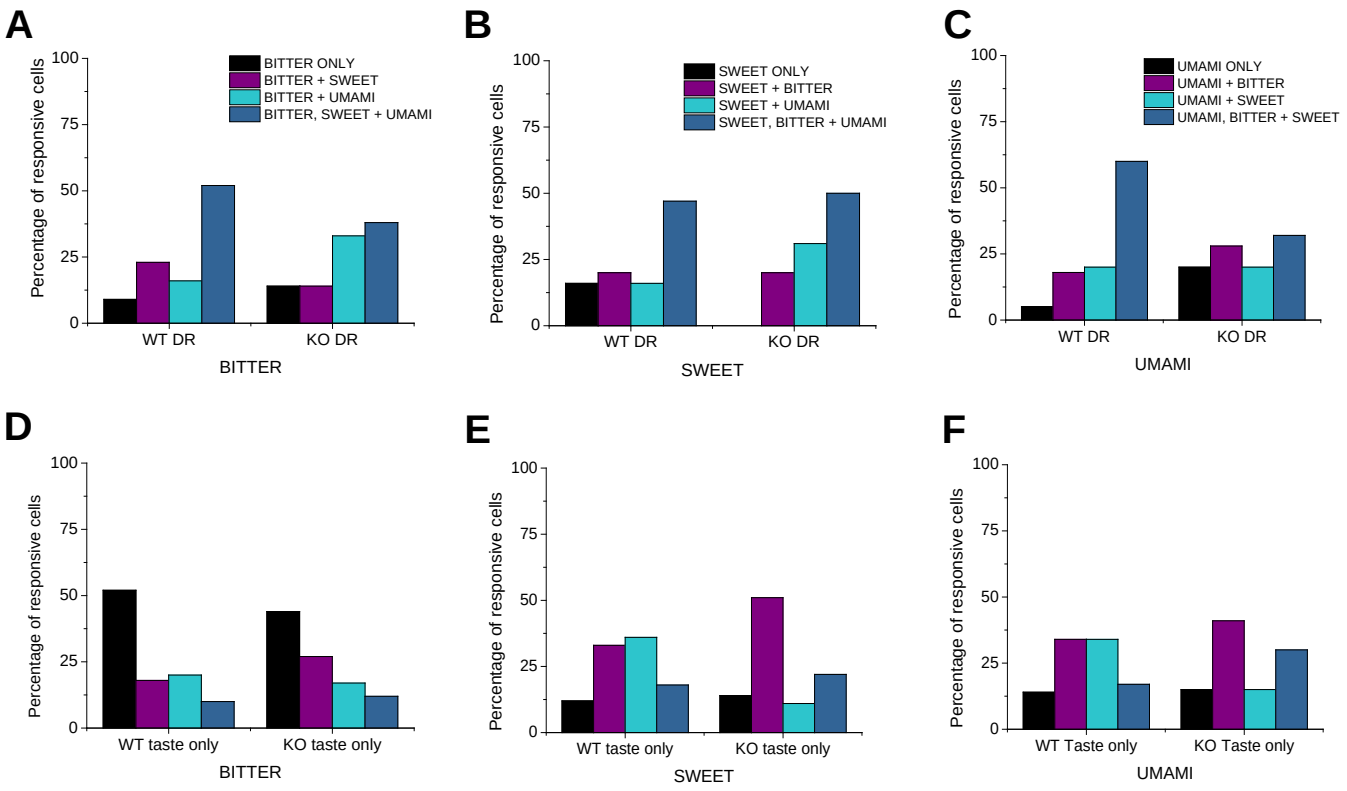

Figure S11. Analyses of the different taste cell populations that responded to taste stimuli. Graphs show the percent of the responses for each taste quality tested. A-C) Response profiles for bitter, sweet and umami stimuli from the DR taste cells in WT (n=29 mice, 62 cells) and IP_3R3-KO (n=18 mice, 31 cells) mice. Taste cells that were stimulated with bitter, sweet and umami stimuli as well as 50mM KCl and responded to at least one of the taste stimuli and KCl were analyzed. The relative percentage of DR taste cells that responded to 1, 2, or 3 taste qualities is shown for each taste quality analyzed. Chi-square analysis with Yate's correction for continuity found no significant differences between the WT and IP_3R3-KO mice for bitter (A), sweet (B), or umami (C) response profiles. The same analysis was applied to taste cells that responded to at least one bitter, sweet or umami stimulus but did not respond to 50mM KCl for WT (n=37 mice, 85 cells) and IP_3R3-KO (n=33 mice, 78 cells) mice. These data are shown for bitter (D), sweet (E), and umami (F). No significant differences were found between WT and IP_3R3-KO mice.